

10282  
NACA TN 3942

NAC  
TN  
394  
3.1

0067138



TECH LIBRARY KAFB, NM

# NATIONAL ADVISORY COMMITTEE FOR AERONAUTICS

TECHNICAL NOTE 3942

INVESTIGATION OF VARIATION IN BASE PRESSURE OVER THE  
REYNOLDS NUMBER RANGE IN WHICH WAKE TRANSITION  
OCCURS FOR NONLIFTING BODIES OF REVOLUTION  
AT MACH NUMBERS FROM 1.62 TO 2.62

By Vernon Van Hise

Langley Aeronautical Laboratory  
Langley Field, Va.



Washington

January 1957

## NATIONAL ADVISORY COMMITTEE FOR AERONAUTICS

  
0067138

## TECHNICAL NOTE 3942

INVESTIGATION OF VARIATION IN BASE PRESSURE OVER THE  
REYNOLDS NUMBER RANGE IN WHICH WAKE TRANSITION  
OCCURS FOR NONLIFTING BODIES OF REVOLUTION  
AT MACH NUMBERS FROM 1.62 TO 2.62

By Vernon Van Hise

#### SUMMARY

An investigation has been made to determine Reynolds number and Mach number effects upon the base pressure of a nonlifting ogival body of revolution over the Reynolds number range in which wake transition occurs. The tests covered a Reynolds number range of approximately 20,000 to 10,000,000 and a Mach number range of 1.62 to 2.62. The results were compared with previous base-pressure data and also with the qualitative theoretical predictions of Crocco and Lees. Throughout the realm of wake transition the base pressure was found to vary with both Reynolds number and Mach number in the same qualitative manner as given by the theory of Crocco and Lees.

#### INTRODUCTION

The problem of predicting base pressure is one of prime importance at moderate supersonic speeds in that base pressure can produce a large portion of the total drag. A number of studies have been made to establish methods for the prediction of base pressure. Of these studies, references 1, 2, and 3 have, perhaps, received most attention in that they present semiempirical and wholly theoretical analyses of base pressure which give satisfactory quantitative (refs. 1 and 2) and promising qualitative (ref. 3) results and indicate the flow mechanisms taking place in the wake. The methods presented in references 1 and 2 permit estimation of the base pressure when the boundary layer on the body ahead of the base is turbulent. Reference 3 presents the only analysis presently available that deals with the prediction of base pressure over the entire Reynolds number range, including that in which wake transition occurs.

In the analysis of reference 3, Crocco and Lees have treated the complex flow at the base of a two-dimensional body by use of their mixing

theory in which mixing, or the transport of momentum from the outer nearly isentropic stream to the dissipative flow region of the wake, is considered to be the fundamental process in determining the pressure rise that can be supported by the flow within the wake. The pressure-rise concept is also the basis of the analogy between base-pressure phenomena and a separated boundary layer established in reference 2 for turbulent boundary layers. As of now the Crocco-Lees analysis has not been evaluated qualitatively for the model of their analysis (two-dimensional base), but the analysis has given satisfactory qualitative predictions for bodies of revolution of the base-pressure variation with Reynolds number (based on model length) for laminar, turbulent, and transitional wakes. Transitional wakes and the Reynolds number range in which wake transition occurs are the particular concern of the present investigation.

Some of the experimental data showing Reynolds number effects upon base pressure in the realm of wake transition have been given by Chapman, Bogdonoff, and Kavanau in references 1, 4, 5, and 6. At a Mach number of 2.0 Chapman made tests over a Reynolds number range from 400,000 to 10,000,000, whereas at a Mach number of 2.95 Bogdonoff varied the Reynolds number from 600,000 to 18,000,000. Both sets of data are in qualitative agreement with theory; that is, the base pressure first decreased rapidly with increasing Reynolds number largely because of the increasing amount of turbulent flow within the wake, and then, after reaching a minimum, began to increase slightly because of the forward movement of the transition point upon the body. Kavanau gave verification of the maximum which exists in the basic base-pressure curve as presented by Crocco and Lees by testing in the Reynolds number range from 45,000 to 400,000 at a Mach number of 2.84. The results of Kavanau's studies of sting interference and base pressure at both intermediate and low Reynolds numbers (refs. 5 and 6), coupled with the Crocco-Lees analysis, indicate that the maximum in base pressure does not correspond to an entirely laminar wake; rather, transition begins to occur in the wake at a Reynolds number lower than that corresponding to the maximum in base pressure. At Mach numbers of 2 and 4, and with Reynolds number ranges of 159 to 800 and 920 to 7,400, respectively, Kavanau found that base pressures decreased with decreasing Reynolds numbers when the wake contained completely laminar flow; that is, the transition point occurred downstream of the wake trailing shock. This type of variation is as predicted by Crocco and Lees for completely laminar flow; however, the assumptions of their theory were not intended to cover these extremely low Reynolds numbers.

The purpose of this paper is to present the results of a wind-tunnel study of base pressures upon nonlifting bodies of revolution in the Reynolds number range in which wake transition occurs. The realm of wake transition is usually associated with missiles and airplanes flying at high altitudes. For instance, a projectile 10 feet long and traveling

at a Mach number of 2 at an altitude of 35 miles might have entered the completely laminar wake-flow regime and might have approached this regime from one of completely turbulent wake flow. Previous base-pressure studies have obtained data at one or two Mach numbers and over Reynolds number ranges which cover portions of the wake transition realm. The data of these studies cannot be easily compared or extrapolated in order to get quantitative variations of base pressure with Mach number over the full Reynolds number range of wake transition because of the various differences in the investigations such as model shape, model smoothness, and airstream turbulence levels. In an attempt to obtain such information, the present tests were carried out at Mach numbers from 1.62 to 2.62 and over a Reynolds number range of approximately 20,000 to 10,000,000.

## SYMBOLS

$C_{p,b}$	base pressure coefficient referred to free-stream conditions, $\frac{p_b - p}{q}$
d	sting diameter
D	model diameter at base
$l_s$	sting length
$l_m$	model length
M	free-stream Mach number
$M_{nom}$	nominal test-section Mach number
p	free-stream static pressure
$p_b$	base pressure
$P_t$	stagnation pressure in stagnation chamber
$p_t'$	stagnation pressure behind normal shock
q	free-stream dynamic pressure, $\frac{\gamma}{2} p M^2$
r	radius defining ogival contour of model

R            Reynolds number based on model length

$\left(\frac{l_s}{D}\right)_{cr}$     critical sting-length ratio

$\gamma$         ratio of specific heats for air, 1.4

## APPARATUS

### Wind Tunnel and Auxiliary Equipment

The Langley 9-inch supersonic tunnel is a continuous-operation, closed-circuit type in which the pressure, temperature, and humidity of the enclosed air can be regulated. Different test Mach numbers are provided by interchangeable nozzle blocks which form test sections approximately 9 inches square. Eleven fine-mesh turbulence-damping screens are installed in the relatively large-area settling chamber ahead of the supersonic nozzle. The turbulence level of the tunnel, based on the turbulence-level measurements presented in reference 7, is considered low. A schlieren optical system is provided for qualitative flow observations.

The static pressure  $p$  and the base pressure  $p_b$  were measured by means of three precision pressure gages having the pressure ranges 0 to 20 millimeters mercury, 0 to 50 millimeters mercury, and 0 to 100 millimeters mercury, all pressures being absolute. Pressures in excess of 100 millimeters mercury and all other test pressures were obtained by means of mercury manometers.

### Models

A photograph of all the models is given in figure 1, and in figure 2 a drawing of a typical model is shown together with the pertinent dimensions of all the models. The models, all of which are similar, are ogival bodies of revolution having a fineness ratio  $\frac{l_m}{D}$  of 8. The ratio of sting diameter to model diameter was held constant at  $\frac{d}{D} = 0.4$ . The support stings had varying  $\frac{l_s}{D}$  ratios in order that interference effects could be minimized. A discussion of relative sting size and its effects upon base pressure is given in the section on sting-support interferences. Base-pressure orifices were obtained by drilling holes on the periphery of the sting in the plane of the model base. Four orifices,  $90^\circ$  apart,

were drilled on the stings of all models except the smallest, on which only two orifices, diametrically opposite, were drilled because of size limitations. Base pressures were obtained by means of tubes connecting the hollow sting and support system to the pressure gages.

The models were constructed of stainless steel and varied in length  $l_m$  from 0.4 to 10 inches. Measured dimensions of the models were within 0.003 inch of the values specified in figure 2. The initial finish of the model surfaces was obtained by standard lathe-machining and lathe-polishing procedures, and a more highly finished surface was attained by polishing with jewelers' rouge. (Similar polishing has been found in previous studies to give a surface roughness of about 8 rms microinches.) Model surfaces were touched up with jewelers' rouge before each test to remove any dulling which may have been incurred in the previous test because of particles carried in the wind stream. Before testing, finger-prints and any other foreign matter which may have collected on the models were removed. These efforts to make the models as polished and clean as possible are essential in obtaining consistent base-pressure data, inasmuch as transition is known to be very sensitive to model surface conditions, and it is upon the degree of wake transition that the value of base pressure depends.

#### TESTS

For this investigation the wind tunnel was operated at stagnation pressures which varied from 3 inches mercury absolute to 4 atmospheres absolute and with stagnation temperatures between 60° F and 110° F. Throughout the tests the dew point was kept sufficiently low to insure negligible effects of condensation. Periodic schlieren observations were made of the flow pattern to determine whether any disturbances were affecting the region of the model wakes. The models were maintained as closely as possible at a condition of zero pitch and zero yaw with reference to the tunnel side walls and center line, respectively.

Tests were conducted at the nominal test-section Mach numbers of 1.62, 1.94, 2.22, 2.41, and 2.62. All models were tested at each Mach number with the exception of the 10-inch model which was not tested at the Mach number 1.62, because its reflected bow wave intersected the wake at the base of the model and thus caused unreliable base-pressure readings.

During each test the independent parameter Reynolds number was varied by regulating the tunnel stagnation pressure, and base-pressure data were taken for each model from the minimum up to the maximum attainable stagnation pressure. This procedure gave base-pressure readings

within various Reynolds number ranges, depending on model length, with considerable overlapping of the Reynolds numbers for the various models so that scale effects could be ascertained. The overall range of Reynolds numbers varied from approximately 20,000 to 10,000,000; thus, base-pressure data were obtained over most of the, if not the entire, Reynolds number range in which wake transition occurs.

Past investigations in supersonic wind tunnels have shown that the scale of the flow (Reynolds number per unit length) may have a significant effect upon the Reynolds number at which transition moves onto a body. For the Langley 9-inch supersonic tunnel, several investigations (see ref. 8, for example) indicate that this transition Reynolds number increases with increasing stagnation pressure by a factor of about two for the range of stagnation pressures of this investigation. No attempt is made in this investigation to evaluate the effect that scale of the flow might have upon wake transition and, therefore, upon base pressure; however, some influence on overall scale effects would be expected.

#### INTERPRETATION AND REDUCTION OF DATA

##### Tunnel Mach Number Variation

The thickness of the boundary layer on the wind-tunnel walls is a function of the stagnation pressure and increases considerably at the lower stagnation pressures. Corresponding to this variation in boundary-layer thickness is an effective change in nozzle contour that produces a varying Mach number, a varying loss of stagnation pressure between the stagnation chamber and the test section, and a change in test-section static pressure that results from both the change in Mach number and the loss in stagnation pressure. Because of the sensitiveness of base pressure to Mach number, efforts were made to determine the true Mach number, as opposed to the nominal test-section Mach number, at that position along the center line of the wind tunnel where the model base was located. Inasmuch as the loss of stagnation pressure was found to increase considerably at the lower stagnation pressures and to assume significant proportions, both a static-pressure survey and a pitot-tube survey were obtained at the location of the model base over the entire range of stagnation pressures and for all nominal Mach numbers.

The data representing the variation of the ratio of static pressure to stagnation pressure  $p/p_t$  with stagnation pressure  $p_t$  are shown in figure 3, and those data representing the variation of the ratio of pitot pressure to stagnation pressure  $p_t'/p_t$  with stagnation pressure  $p_t$  are shown in figure 4. From these two pressure surveys, the ratio of the static pressure  $p$  to the pitot pressure  $p_t'$  can be

obtained for any given tunnel stagnation pressure  $p_t$ ; these ratios determine the corresponding Mach number over the full range of stagnation pressures. Curves showing the variation of Mach number with stagnation pressure are given in figure 5. In each of these figures (figs. 3 to 5) it is seen that the largest and most rapid variations occur at the low stagnation pressures. At a particular nominal Mach number, these figures together indicate a significant loss of stagnation pressure through the supersonic nozzle at the lower stagnation pressures in that, contrary to isentropic conditions,  $p_t'/p_t$  decreases with decreasing Mach number.

The trends of the curves of figure 5 show that Mach number decreases slowly with decreasing stagnation pressure until  $p_t$  equals approximately  $1/3$  atmosphere where a rapid decrease in Mach number occurs as the stagnation pressure is decreased. All values of Reynolds number and base-pressure coefficient have been computed for the true test conditions as determined by these surveys.

#### Sting-Support Interference

Inasmuch as the models of this investigation were sting supported, consideration must be given to possible sting-support effects upon the measured values of base pressure. Sting-support effects upon the measured values of base pressure with regard to both sting length and sting diameter are presented in references 1, 5, and 9. It was found that, as long as the boundary layer ahead of the base is not fully turbulent, the critical sting-length ratio  $\left(\frac{l_s}{D}\right)_{cr}$  (i.e., the ratio above

which the base pressure is not significantly affected by sting length) varies appreciably with Reynolds number. Kavanau (ref. 5) determined

the variation of  $\left(\frac{l_s}{D}\right)_{cr}$  with Reynolds number for a cone-cylinder body

at a Mach number of 2.84. From Kavanau's plot, presented in figure 6, it is seen that in the Reynolds number range from 45,000 to 400,000 the critical sting-length ratio increases rapidly as the Reynolds number is decreased. Inasmuch as these were the only available data on critical sting lengths in approximately the same Mach number and Reynolds number ranges covered in this investigation, these data and extrapolations of them (dashed portion of curve) were used in determining the sting lengths for the models of the present tests. Figure 7 presents a curve of

$\left(\frac{l_s}{D}\right)_{cr}$  based on Kavanau's data of figure 6 in which the lowest test

Reynolds number for each model was used in finding the necessary critical sting length according to Kavanau's curve. Figure 7 also shows the actual ratio of sting length to model diameter for the model tested, and

it is seen that this ratio has been conservatively chosen, the ratio being somewhat larger than the ratio  $\left(\frac{l_s}{D}\right)_{cr}$  determined by Kavanau's curve.

In references 1 and 9 are given data showing the typical variation of base-pressure coefficient with the ratio of sting diameter to base diameter. In general, these data show a considerable variation of base-pressure coefficient as  $d/D$  varies from 1 to about 0.4 and only a slight variation of base-pressure coefficient as  $d/D$  varies from 0.4 to 0. These data extend into the upper Reynolds number range of wake transition. In the lower Reynolds number range of wake transition Kavanau (ref. 5), using stings with  $d/D$  greater than 0.2, found no significant effects upon base pressure of sting diameter and of orifice location. In view of the foregoing findings on sting-diameter interference and also of necessary sting-strength requirements, the ratio of sting diameter to base diameter was made 0.4. Hence, for this investigation the base pressure should not be greatly affected by sting-diameter interference.

#### Precision of Data

All models were maintained within  $\pm 0.25^\circ$  of zero pitch and yaw with reference to the tunnel side walls and center line, respectively. Past measurements of the flow angularity in the tunnel test section have shown negligible deviations. The indicated location of the model bases, the static probe, and the pitot tube was accurate within  $\pm 0.010$  inch. The maximum error in the base- and static-pressure readings recorded from the precision pressure gages was set at  $\pm 0.5$  percent of the full-scale deflection. The estimated overall accuracies of the main test variables are as follows:

Mach number, M (at 1 atmosphere stagnation pressure) . . . . .	$\pm 0.01$
Reynolds number, R (probable error at $R = 1 \times 10^6$ ) . . . . .	$\pm 0.01 \times 10^6$
Base-pressure coefficient, $C_{p,b}$ . . . . . . . . . . . . . . . . .	$\pm 0.002$

#### RESULTS AND DISCUSSION

##### Variation of Base Pressure With Reynolds Number

Figure 8 presents base-pressure coefficient as a function of Reynolds number for each model at the various nominal Mach numbers. Each data point is based on the true Mach number corresponding to the particular tunnel stagnation pressure; hence, the data points give the base-pressure-coefficient curves along which the Mach number varies. However, the

curves would be negligibly affected by this Mach number change except at the lower Reynolds numbers for each curve where Mach number decreases rapidly as the Reynolds number is decreased.

At the low Reynolds number section of some of the curves of figure 8, a relatively rapid increase in base-pressure coefficient occurs (an increase in absolute base pressure) with decreasing Reynolds number. In order to examine this increase in base-pressure coefficient more closely, figure 9 is presented in which each of the original curves of figure 8 have been redrawn and grouped according to nominal test-section Mach number. The results for the different models overlap each other considerably in Reynolds numbers, and with the exception of the low Reynolds number section of all the curves, the curves of each model are seen to fall reasonably together and indicate no large or consistent scale effects. At the low Reynolds number section of the curves which in figure 8 exhibited the aforementioned relatively rapid increase in base-pressure coefficient with decreasing Reynolds number, there is a tendency for this section of these curves to turn away from the main body of curves. Effects that might be suspected to contribute to such a departure from the mean curve of all the models at the low Reynolds numbers of each model are faulty instrumentation at low pressures, sting-length interference, and rapid Mach number variation along with the flow conditions which accompany it. No faulty behavior of the instrumentation at low pressures could be found. In order to determine whether sting-length interference was present, the 1.8-inch-long model was retested at a nominal Mach number of 2.22 with its sting lengthened about 5 body diameters. Base-pressure coefficients obtained from this test coincided with those from the same model with the original shorter sting and thus indicated an absence of any significant sting-length interference on the results. In the general Reynolds number range where the individual curves depart from the mean curve, the base-pressure coefficient is not very sensitive to changes in Mach number, as is shown in a subsequent section. Hence, this rapid variation in base-pressure coefficient cannot be a direct function of Mach number alone. However, other flow conditions accompanying low tunnel stagnation pressures, which are such as to lower nozzle performance and spoil considerably an idealized isentropic flow as discussed previously, do present a possible explanation for the rapid base-pressure rise as found; scale effects also offer a possible but less probable explanation. Inasmuch as the data points at the low stagnation pressures definitely differ from the trends of the mean proper curve, they were eliminated from the final plots for all models except the smallest model. Data points at the low stagnation pressures were included for the smallest model because this model has no mean curve for comparison and seems to give data with a more rapid variation than the other models at the low stagnation pressures.

Figure 10 presents base-pressure-coefficient data in cross-plotted form with base-pressure coefficient as a function of Mach number at

various constant Reynolds numbers. All possible models and Mach numbers are included in each Reynolds number curve. Except for the smallest model in its lower Reynolds number range and the largest model in its upper Reynolds number range, there was plentiful overlapping of points so that for the majority of curves rather accurate fairings could be obtained. From these curves final plots of base-pressure coefficient as a function of Reynolds number were made with the values of the nominal test-section Mach numbers as parameters. Figure 11, which presents these final base-pressure-coefficient curves, gives the full scope of base-pressure variation with Reynolds number and Mach number of the present investigation. A dividing line has been indicated in the figure and all points to the right of it are considered essentially free of any effects connected with possible poor flow conditions or some other low-pressure phenomena. The sections of the curves to the left of the dividing line contain data only from the smallest model and have been shown for consistency and for possible trends in the variation of base-pressure coefficient. (The data for the smallest model also extend well into the region right of the dividing line.) Inasmuch as these data to the left of the dividing line are at the lower stagnation pressures they might, like the data at the lower stagnation pressures of the larger models, contain some undetermined low-pressure effects. However, inasmuch as these low-pressure data for the smallest model seem to be affected more highly than those of the other models, additional effects may be superimposed on those low-pressure effects present for all the larger models at low stagnation pressures. First, the Reynolds number is such that the flow is beginning to enter the realm of slip flow, slip flow beginning approximately when  $\frac{M}{\sqrt{R}} > 0.01$ , and second, the ratio of

boundary-layer thickness to base diameter has become relatively large. Thus, although this increase in base pressure at the lowest Reynolds numbers is not in agreement with the qualitative predictions of Crocco and Lees, it is well to note that neither of these effects has been accounted for in the theoretical development of Crocco and Lees; further, the Reynolds number effect upon base pressure for Reynolds numbers as low as these is not covered by their mixing theory. On the basis of Kavanau's results at much lower Reynolds numbers (ref. 6), a decrease in base-pressure coefficient would be expected with much further decrease in Reynolds number. The sections of the base-pressure-coefficient curves to the right of the dividing line are in qualitative agreement with the mixing theory as given by Crocco and Lees and give a Reynolds number coverage of wake transition as the wake progresses from an almost entirely laminar wake to a completely turbulent wake at Mach numbers from 1.62 to 2.62. Figure 12 presents the curves of figure 11 in the form of the base-pressure ratio  $p_b/p$ , inasmuch as the theoretical treatment of Crocco and Lees and some of the previous base-pressure data have been so presented.

### Variation of Base Pressure With Mach Number

From the constant Reynolds number curves of figure 10, definite trends of the variation of base-pressure coefficient with Mach number can be observed. At the higher Reynolds numbers where the wake flow is largely if not completely turbulent, the base-pressure coefficient increases rapidly as the Mach number increases. In the Reynolds number region of about 100,000 where the wake is almost completely laminar, the base-pressure coefficient varies only slightly with Mach number. These effects are somewhat analogous to the Mach number effects upon skin-friction coefficient, which, like base-pressure coefficient, depends on the viscous condition of the flow. The condition of the boundary layer on the surface of a body determines the skin-friction coefficient whereas the condition of the wake flow determines the base-pressure coefficient. Each of these coefficients varies only slightly with Mach number when its respective flow condition is laminar, and varies appreciably with Mach number when its respective flow condition is turbulent. All the Reynolds number curves below a Reynolds number of the order of 50,000, dependent upon Mach number as indicated in figure 11, may include some undetermined low-pressure effects and have been included for consistency and to show possible trends which might occur in the realm of completely laminar wake flow or almost so.

Figure 13 presents curves of base-pressure coefficient as a function of Mach number. The lower curve represents a compilation of both free-flight and wind-tunnel data presented in references 1 and 2 and gives base-pressure coefficients for a fully established turbulent boundary layer on the body. Inasmuch as a fully established turbulent boundary layer was not quite reached for all Mach numbers of the present investigation, the upper curve, which gives the minimum base-pressure coefficients reached at each Mach number, is presented for comparison. The difference between the two curves is consistent with the usual increase in base-pressure coefficient occurring in this Mach number range as transition moves from the wake onto the rear of the body and a fully developed turbulent boundary layer occurs on the rear of the body.

Figure 12 indicates that the absolute pressure at the base decreases with increasing Mach number at a constant Reynolds number in the regions of wholly laminar and wholly turbulent wake flow. This decrease is the result of the ability of a higher flow velocity to scavenge a greater portion of the air behind the base and to its ability to sustain in this Mach number range a greater recompression through the wake trailing shock. In the intermediate Reynolds number range from about 500,000 to 3,000,000 where the wake contains both turbulent and laminar flow, the absolute base pressure varies only slightly with Mach number at constant Reynolds numbers. Although higher Mach numbers would still have greater scavenging ability, there is, apparently, in this intermediate Reynolds number range, a change with Mach number in the rate at

which transition moves forward in the wake with increasing Reynolds number that tends to nullify the former effects. Figure 12 also shows that the difference in Reynolds number between that corresponding to the maximum in the base-pressure curves to the right of the dividing line and that corresponding to the knee in the curves at the high Reynolds numbers (a fully turbulent wake) decreases as Mach number increases. This observation may lead to the conclusion that the total range of Reynolds number over which wake transition occurs decreases with increasing Mach number. However, substantiation of this conclusion must await further experimental evidence; for, although the knee in the curves at the high Reynolds numbers is a valid indication of the end of wake transition, the beginning of wake transition does not coincide with the maximum in the curves but occurs at some lower, but as yet undetermined, Reynolds number.

#### General Base-Pressure Phenomena

The complex flow about the base of a two-dimensional body has been analyzed by Crocco and Lees (ref. 3); inasmuch as the data of the present investigation show the same trends which they have predicted theoretically, the analysis seems to be applicable to an axisymmetric body in providing qualitative predictions along with the proper physical concepts. The theory is founded on the premise that viscous mixing in the wake flow is a dominant factor in determining base pressure. Hence, Reynolds number and Mach number are main parameters in base-pressure studies and determine the general condition of the wake, that is, how much of the wake is laminar and how much is turbulent. Also dependent on Reynolds number and Mach number is the boundary-layer thickness at the base of the body, and the combination of boundary-layer thickness at the base, base height, and the amount of viscous mixing determines the base pressure.

The schematic drawing of the test model shown in figure 14 points out some of the flow regimes which concern base-pressure studies. A singularity occurs in the basic differential equation of wake flows as given by Crocco and Lees and indicates that a certain critical point exists at a position in the region of the narrowest part of the wake at about the same place where the trailing shock originates. This point has the characteristic that disturbances produced in the wake downstream of this point are not able to affect the base pressure. This point fluctuates up and down the wake as the Reynolds number is changed and thus indicates the necessary variation in critical sting length as previously discussed. The condition of the flow in the region designated as the critical wake region together with the thickness of the boundary layer at the base of the body determines the base pressure.

As seen in figure 12, the typical base-pressure curve contains a maximum and a minimum. Proceeding with this figure from low to high

Reynolds number, wake transition affects each base-pressure curve in the following manner: The underlying consideration is that the greater the viscous mixing action occurring in the wake the more high-speed flow which can be enveloped in the critical wake region, and hence a greater pressure rise through the trailing shock can be supported by the wake flow and results in a lower base pressure. At first the wake is all or nearly all laminar and, as the Reynolds number is increased, the effect is to decrease the laminar-mixing coefficient and to decrease the boundary-layer thickness at the base, each condition having an opposite effect on base pressure. However, the decrease in laminar mixing is the overpowering factor and, therefore, the base pressure increases with increasing Reynolds number. As the Reynolds number is further increased, transition has crept far enough into the critical wake region so that the turbulent part of the wake (turbulent flow having 5 to 10 times the mixing rate of laminar flow) counteracts the continually poorer mixing of the laminar part and eventually causes a net increase in the total mixing action of the wake. Hence, a maximum in base pressure is reached, followed by a continued fall in base pressure as transition moves upstream in the wake and the turbulent mixing increases. A decrease in base pressure continues until wake transition occurs just at the base. Now as the Reynolds number is further increased the viscous mixing within the wake is not significantly increased and the thickness of the boundary layer at the base becomes an important factor in the determination of base pressure. As transition moves forward onto the body, the initial effect is to cause a thickening of the boundary layer at the base; hence, the minimum in base pressure is followed by a rise in base pressure. The Reynolds number range of the present tests moves the transition point this far upstream, that is, the highest Reynolds numbers give a condition of completely turbulent wake flow and a turbulent boundary layer on the body. It is known from previous studies (ref. 2, for example) that once a fully developed turbulent boundary layer exists on the body, the change in base pressure with Reynolds number is small.

#### Comparison With Previous Data

Figure 15 compares base-pressure data obtained in the range of wake transition in past investigations with data of the present tests. All these past investigations were made with cone-cylinder bodies of revolution as opposed to the ogival models of the present tests. In addition, the fineness ratios were considerably less than 8, Chapman using a fineness ratio of 5 and Bogdonoff and Kavanau, a fineness ratio of 3.4. These differences in test conditions together with differences in any factors to which wake transition is sensitive, in particular differences in airstream turbulence levels, make it difficult to obtain a meaningful quantitative comparison. All the previous test curves are seen to be shifted to the left of the present test curves, a large part of the shift probably being due to the differences in fineness ratio, body shape,

and turbulence levels. In keeping with the Mach number variations of the maximum and the minimum base-pressure ratios of the present tests, the curves from previous tests fall rather well into their proper levels of magnitude. This general trend would appear to indicate that the Mach number and the static pressure just ahead of the base of the variously shaped models were sufficiently close to free-stream values that model shape did not greatly affect the relative values of maximum and minimum base-pressure ratio as attained through wake transition.

#### CONCLUDING REMARKS

An investigation has been made to determine the effects of Mach number and Reynolds number upon the base pressure of an ogival body of revolution over the Reynolds number range in which wake transition occurs. The Mach number varied from 1.62 to 2.62 and the Reynolds number range of the tests was approximately 20,000 to 10,000,000 based on body length.

The variation of base-pressure coefficient with Reynolds number and Mach number was found to agree qualitatively with theoretical predictions of Crocco and Lees. In particular, the Reynolds number range investigated carried the absolute base pressure from a maximum which corresponds to an almost completely laminar wake to a minimum which corresponds to a completely turbulent wake. The base-pressure coefficient was found to vary appreciably with Mach number when the wake contained mostly turbulent flow and was found to vary only slightly with Mach number when the wake contained mostly laminar flow.

Langley Aeronautical Laboratory,  
National Advisory Committee for Aeronautics,  
Langley Field, Va., November 15, 1956.

## REFERENCES

1. Chapman, Dean R.: An Analysis of Base Pressure at Supersonic Velocities and Comparison With Experiment. NACA Rep. 1051, 1951. (Supersedes NACA TN 2137.)
2. Love, Eugene S.: Base Pressure at Supersonic Speeds on Two-Dimensional Airfoils and on Bodies of Revolution With and Without Fins Having Turbulent Boundary Layers. NACA TN 3819, 1957. (Supersedes NACA RM L53C02.)
3. Crocco, Luigi, and Lees, Lester: A Mixing Theory for the Interaction Between Dissipative Flows and Nearly Isentropic Streams. Jour. Aero. Sci., vol. 19, no. 10, Oct. 1952, pp. 649-676.
4. Bogdonoff, Seymour M.: A Preliminary Study of Reynolds Number Effects on Base Pressure at  $M = 2.95$ . Jour. Aero. Sci., vol. 19, no. 3, Mar. 1952, pp. 201-206.
5. Kavanau, L. L.: Results of Some Base Pressure Experiments at Intermediate Reynolds Numbers With  $M = 2.84$ . Jour. Aero. Sci., vol. 21, no. 4, Apr. 1954, pp. 257-260, 274.
6. Kavanau, L. L.: Base Pressure Studies in Rarefied Supersonic Flows. Tech. Rep. No. HE-150-125. (Ser. 20, Issue 101, Contract N7-onr-295-Task 3), Univ. of California Inst. Eng. Res., Nov. 1, 1954.
7. Love, Eugene S., Coletti, Donald E., and Bromm, August F., Jr.: Investigation of the Variation With Reynolds Number of the Base, Wave, and Skin-Friction Drag of a Parabolic Body of Revolution (NACA RM-10) at Mach Numbers of 1.62, 1.93, and 2.41 in the Langley 9-Inch Supersonic Tunnel. NACA RM L52H21, 1952.
8. Grigsby, Carl E., and Ogburn, Edmund L.: Investigation of Reynolds Number Effects for a Series of Cone-Cylinder Bodies at Mach Numbers of 1.62, 1.93, and 2.41. NACA RM L53H21, 1953.
9. Love, Eugene S.: A Summary of Information on Support Interference at Transonic and Supersonic Speeds. NACA RM L53K12, 1954.

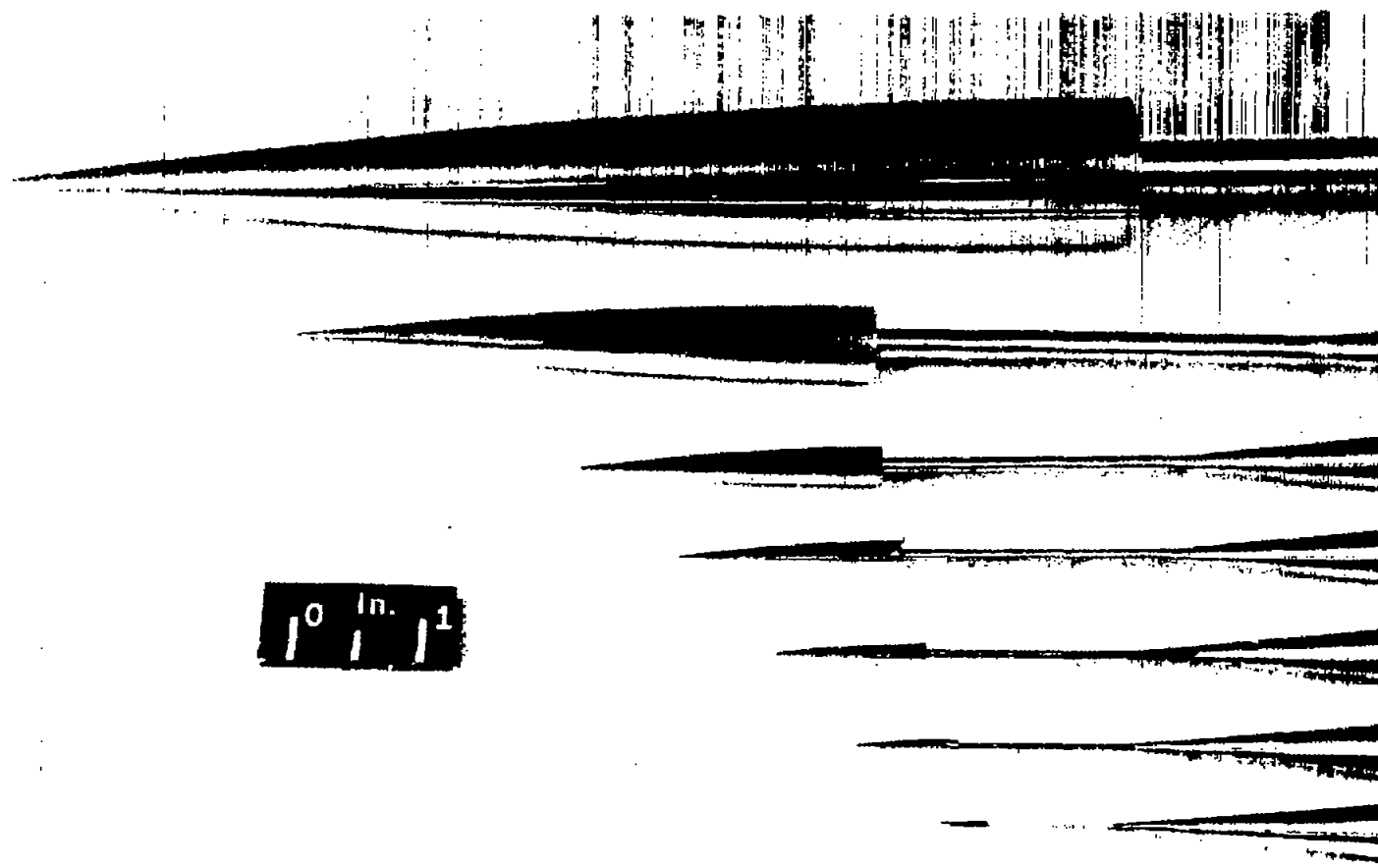
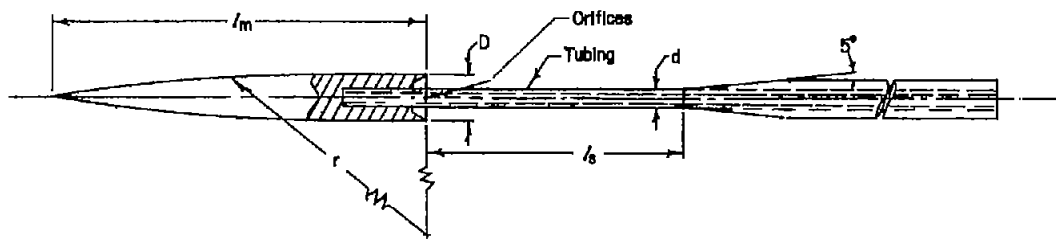


Figure 1.- Photograph of test models.

L-92850



Detail dimensions

$l_m$	D	r	$l_s$	d	Orifices
10.00	.250	80.32	7.00	.500	4-.020 diam.
5.00	.625	40.16	3.75	.250	4-.020
2.50	.312	20.08	2.44	.125	4-.020
1.80	.225	14.46	2.06	.090	4-.020
1.80	.225	14.46	3.15	.090	4-.020
1.20	.150	9.64	1.62	.060	4-.020
.80	.100	6.43	1.25	.040	4-.020
.40	.050	3.21	.81	.020	2-.004

\* Some model with increased sting length.

Figure 2.- Drawing of typical test model. All linear dimensions are in inches.

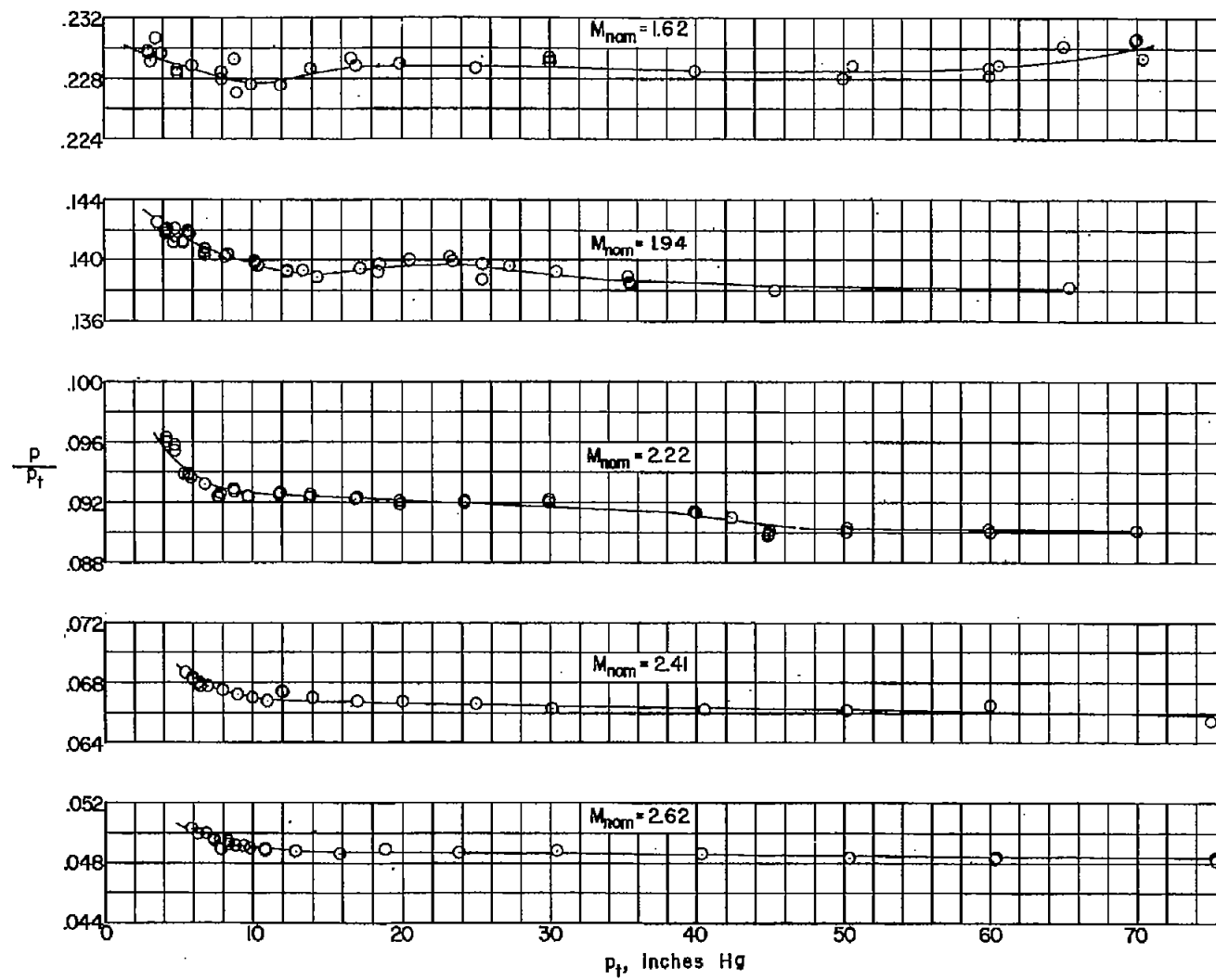


Figure 3.- Variation of ratio  $p/p_t$  with tunnel stagnation pressure.

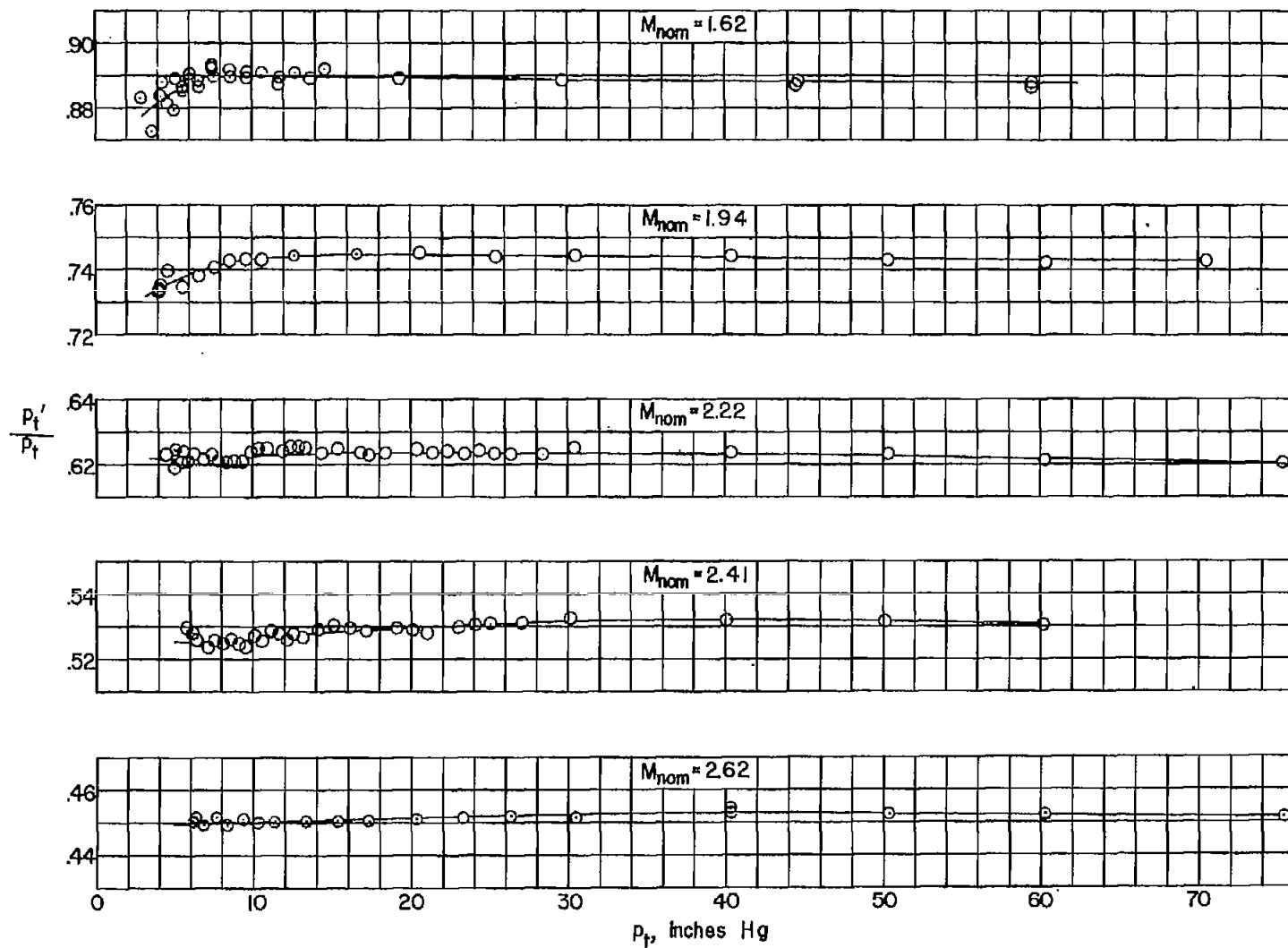


Figure 4.- Variation of ratio  $p_t'/p_t$  with tunnel stagnation pressure.

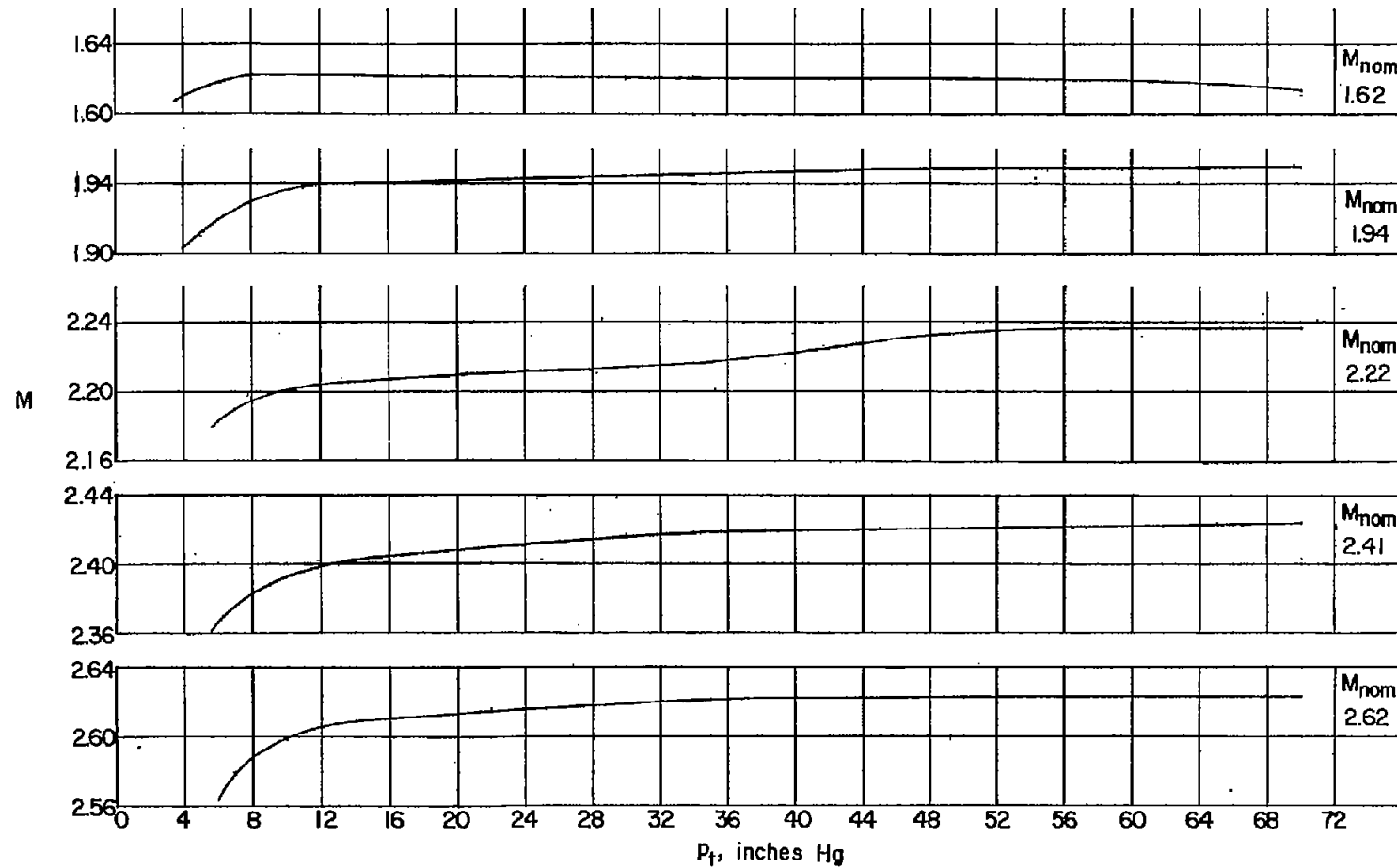


Figure 5.- Effect of tunnel stagnation pressure upon Mach number.

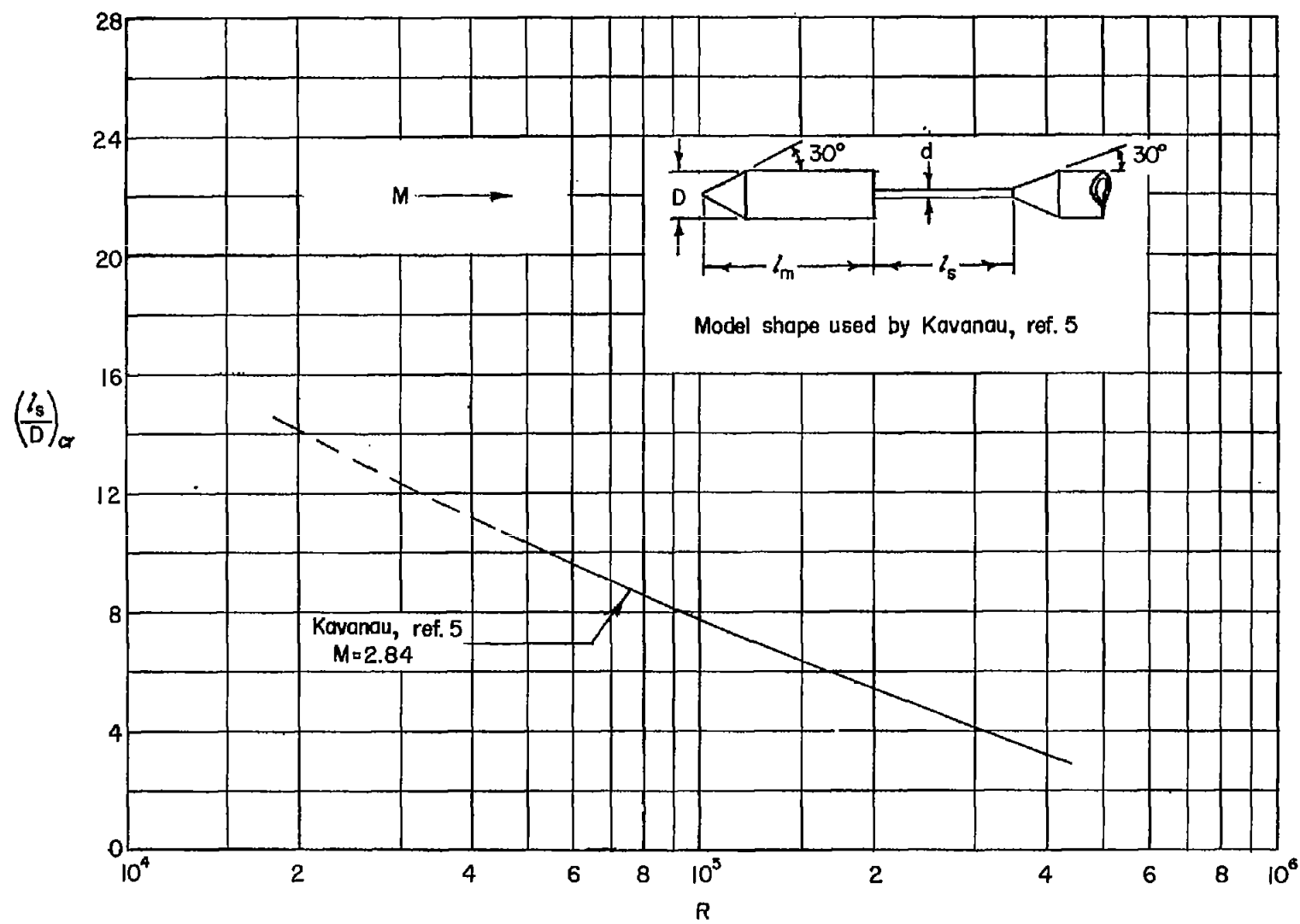


Figure 6.- Effect of Reynolds number upon critical sting-length ratio.

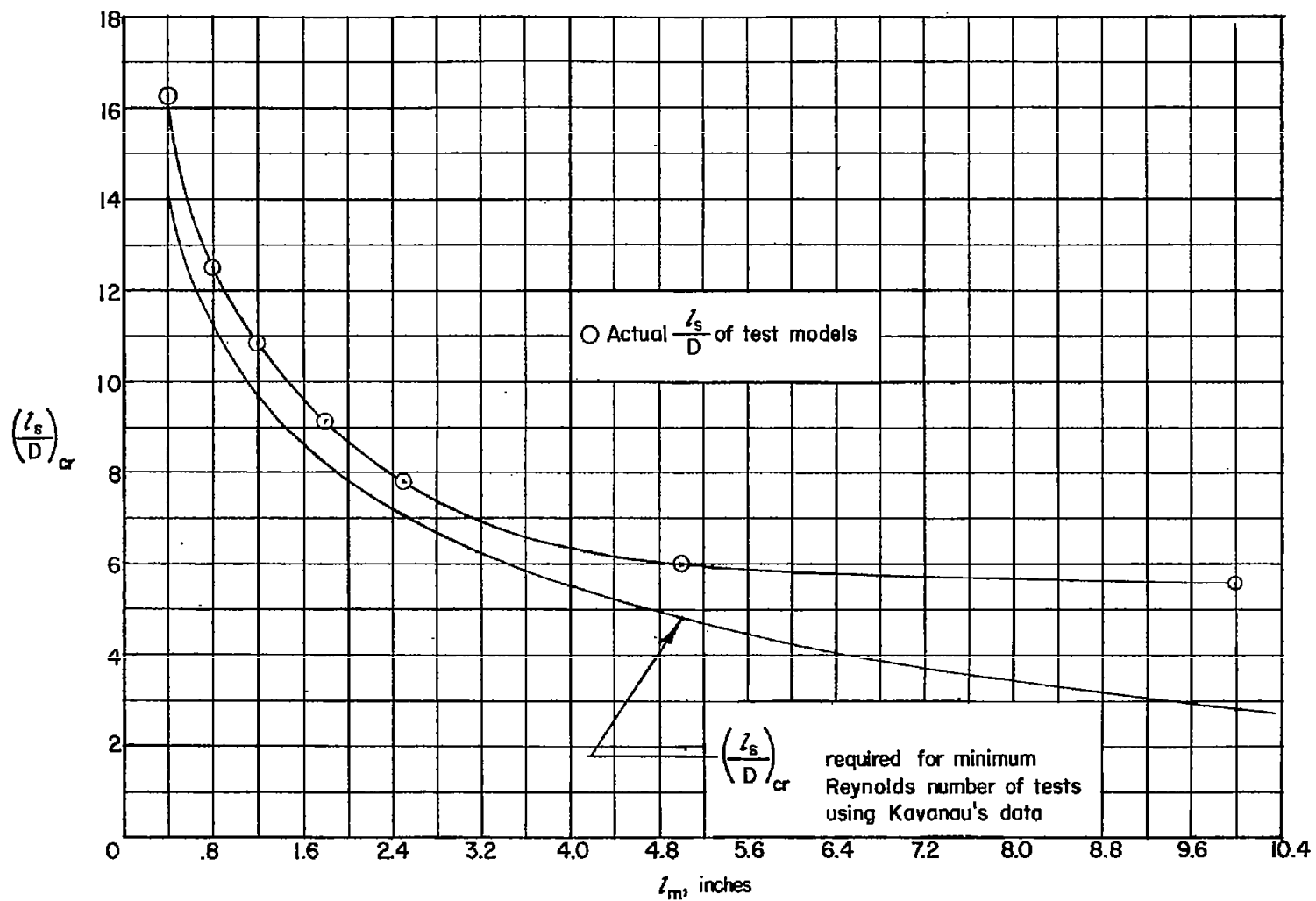


Figure 7.- Values of critical sting-length ratio as affected by model length through parameter Reynolds number.

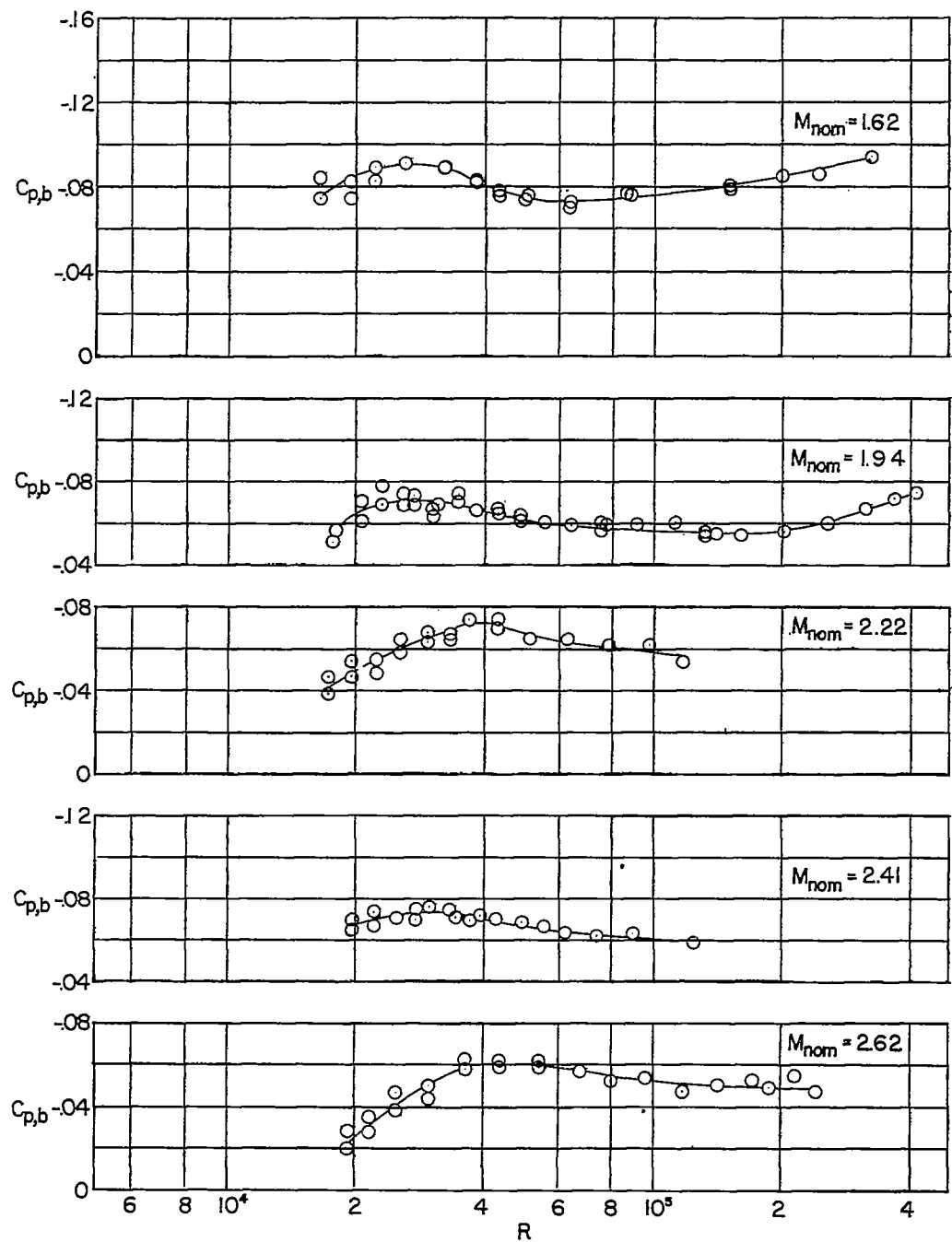
(a)  $l_m = 0.4$  inch.

Figure 8.- Variation of base-pressure coefficient with Reynolds number.

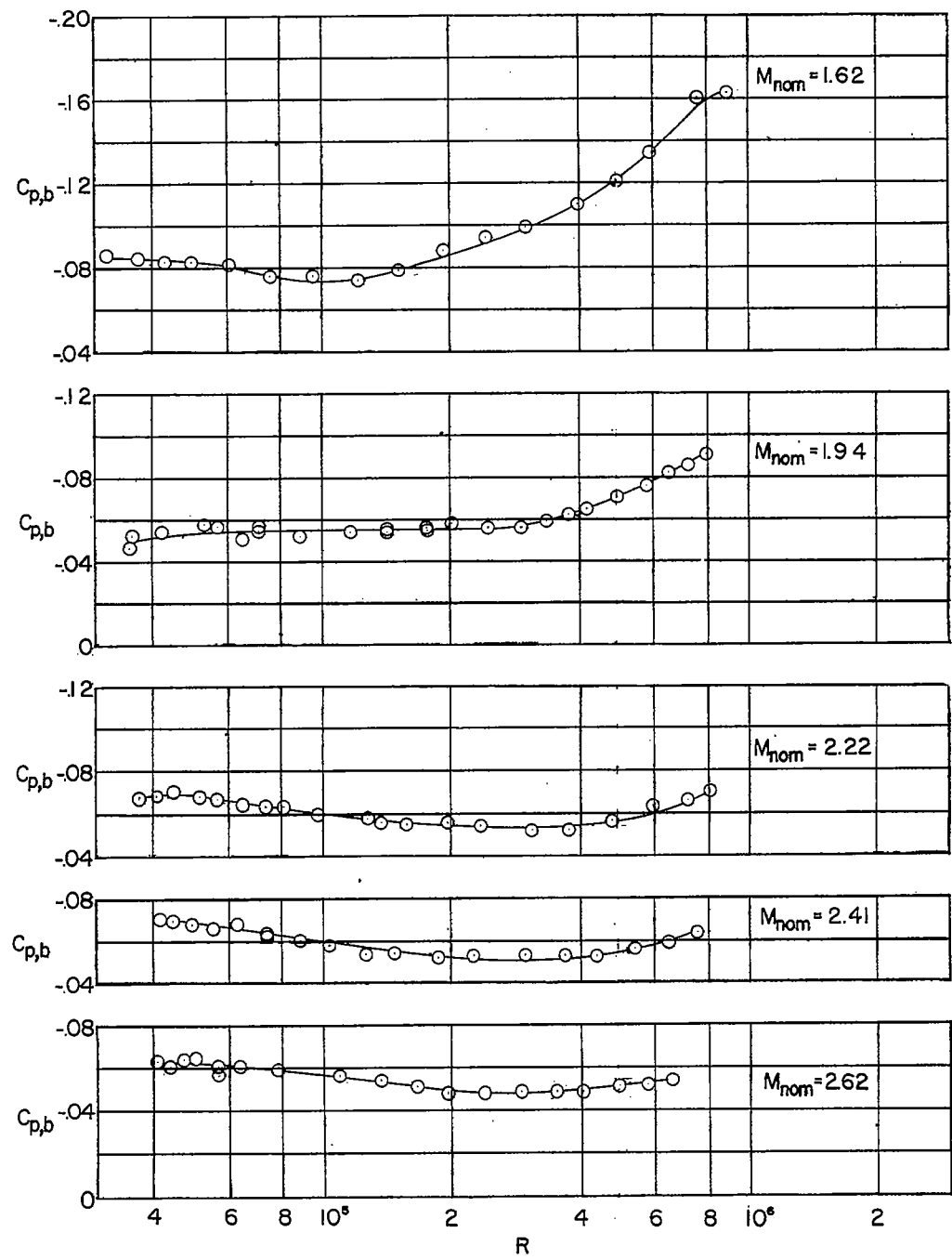
(b)  $t_m = 0.8$  inch.

Figure 8.- Continued.

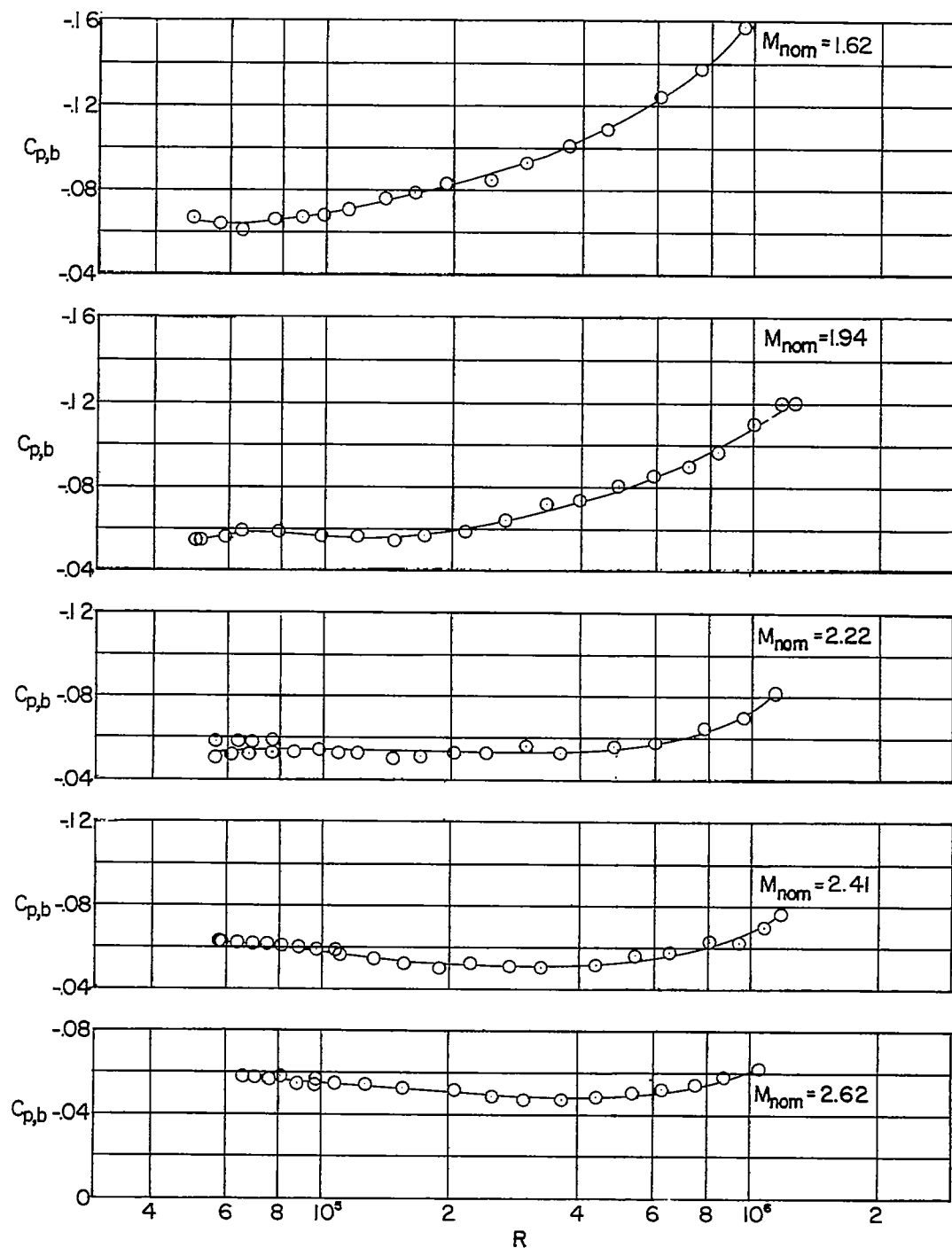
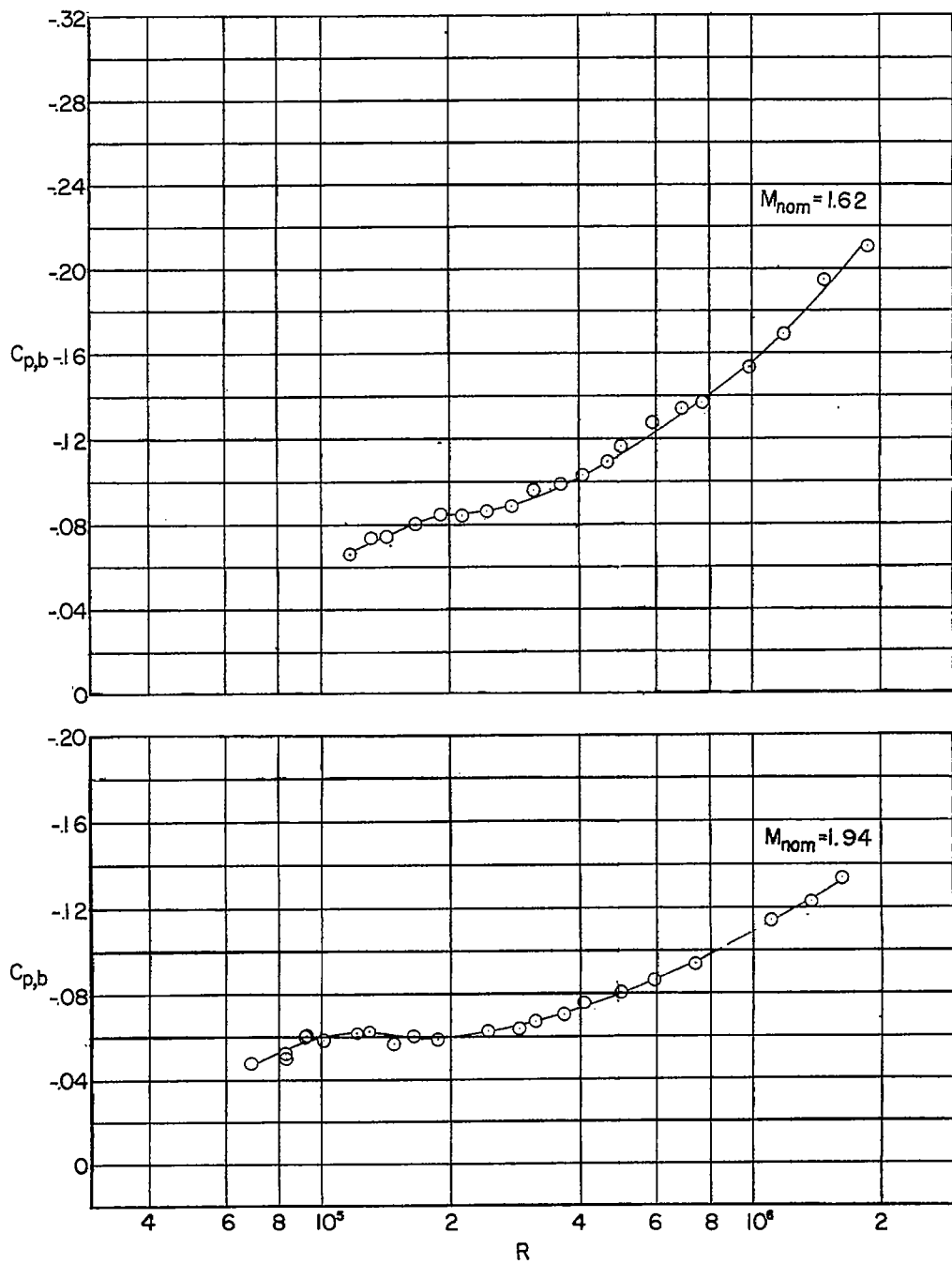
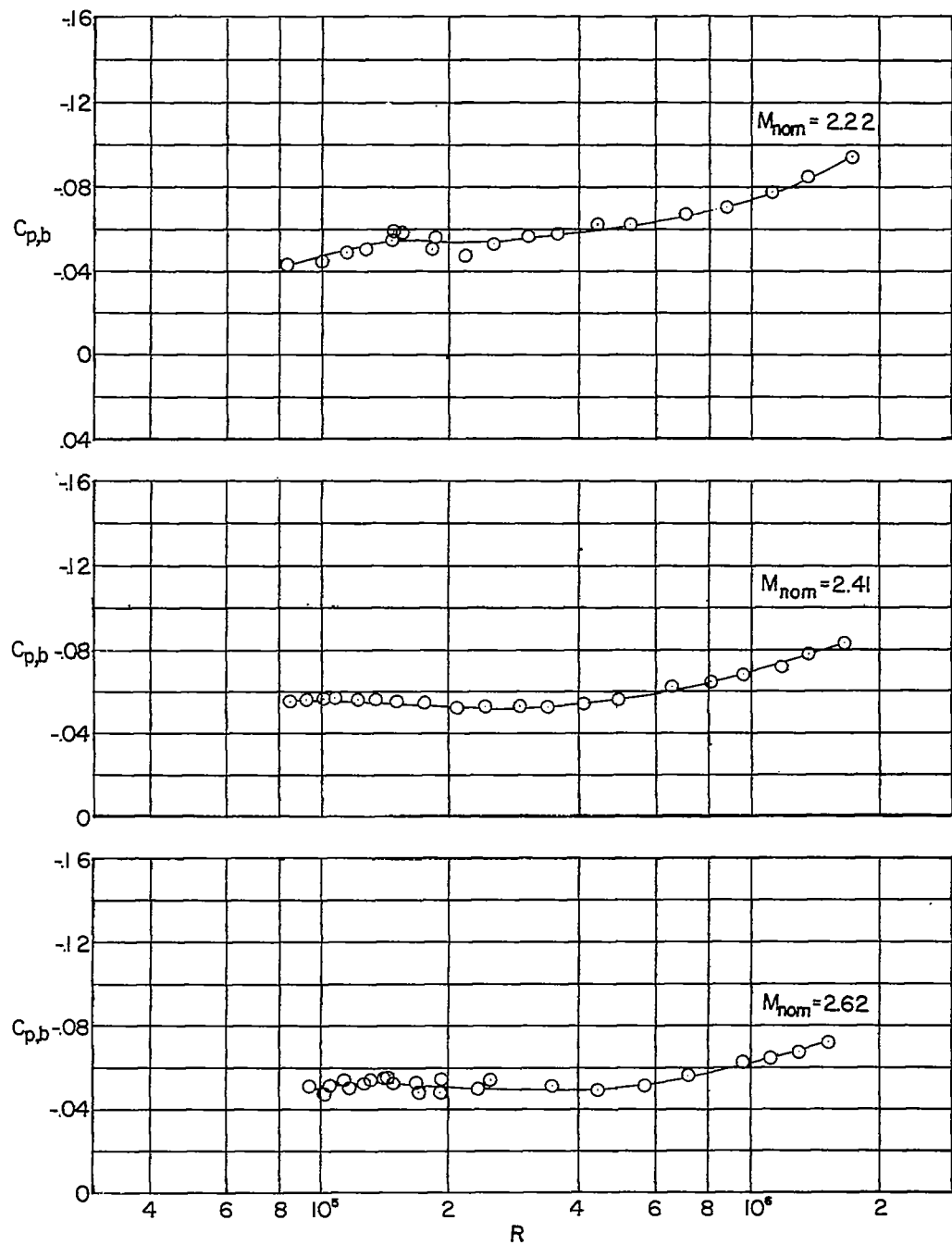
(c)  $l_m = 1.2$  inches.

Figure 8.- Continued.



(d)  $l_m = 1.8$  inches.

Figure 8.- Continued.



(d) Concluded.

Figure 8.- Continued.

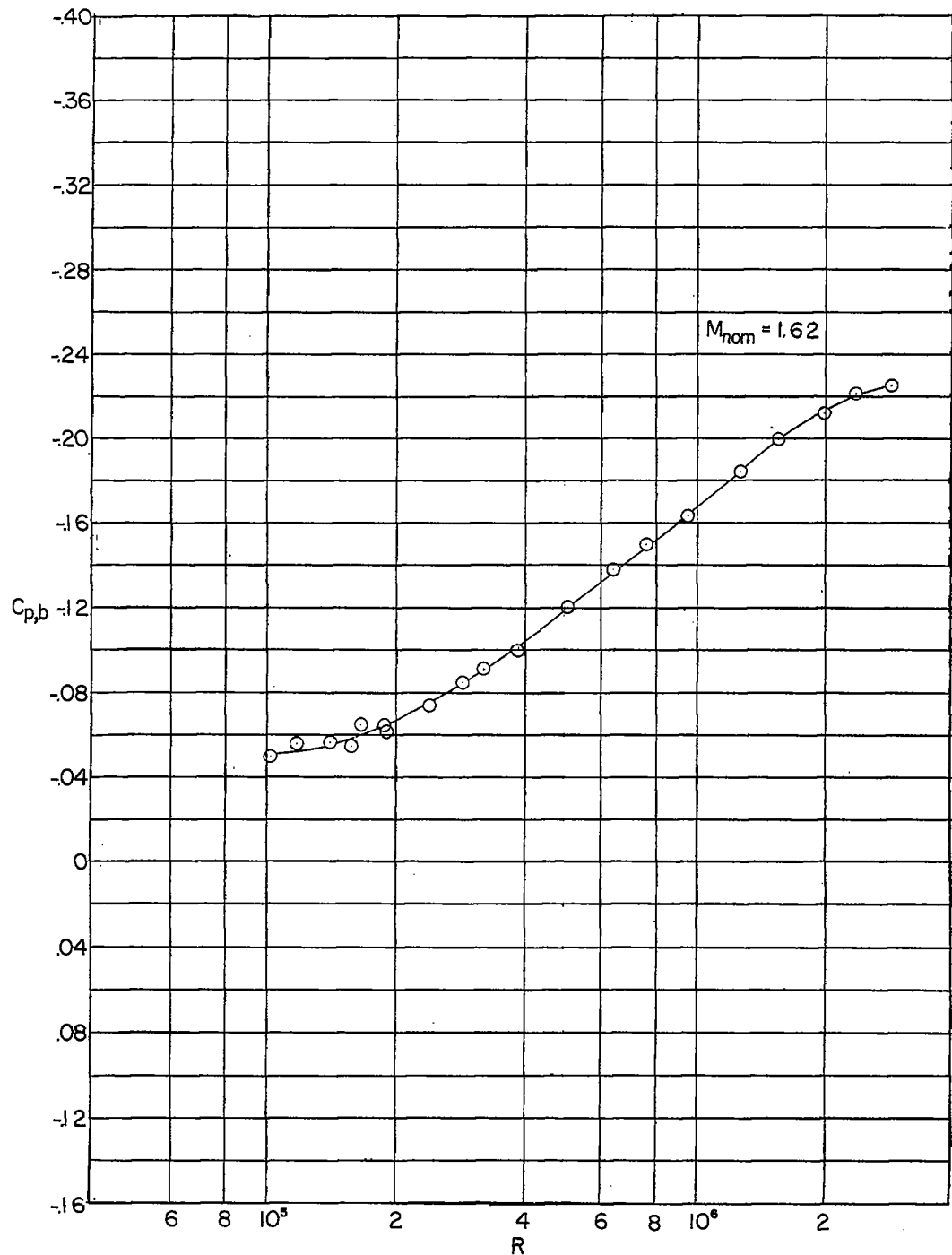
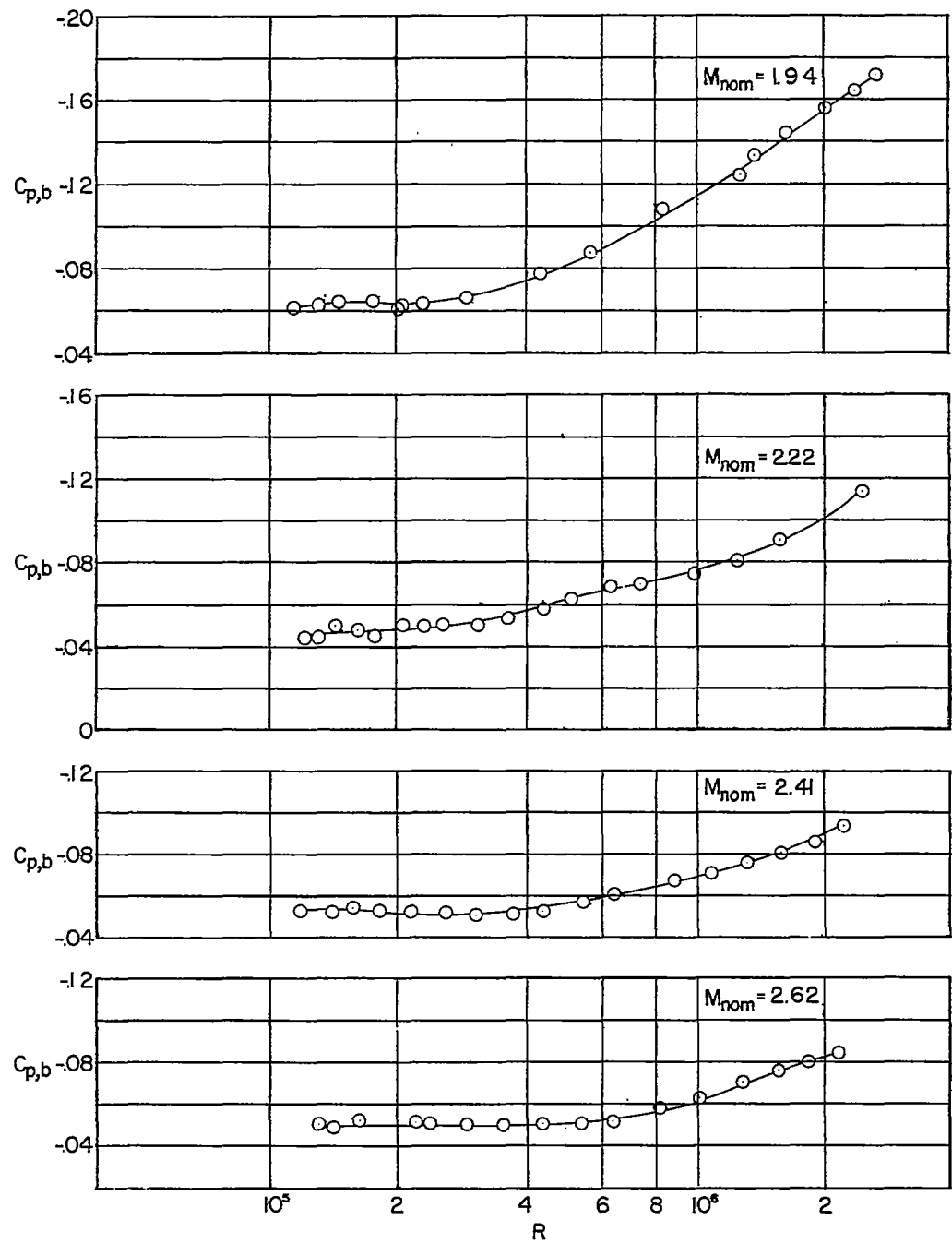
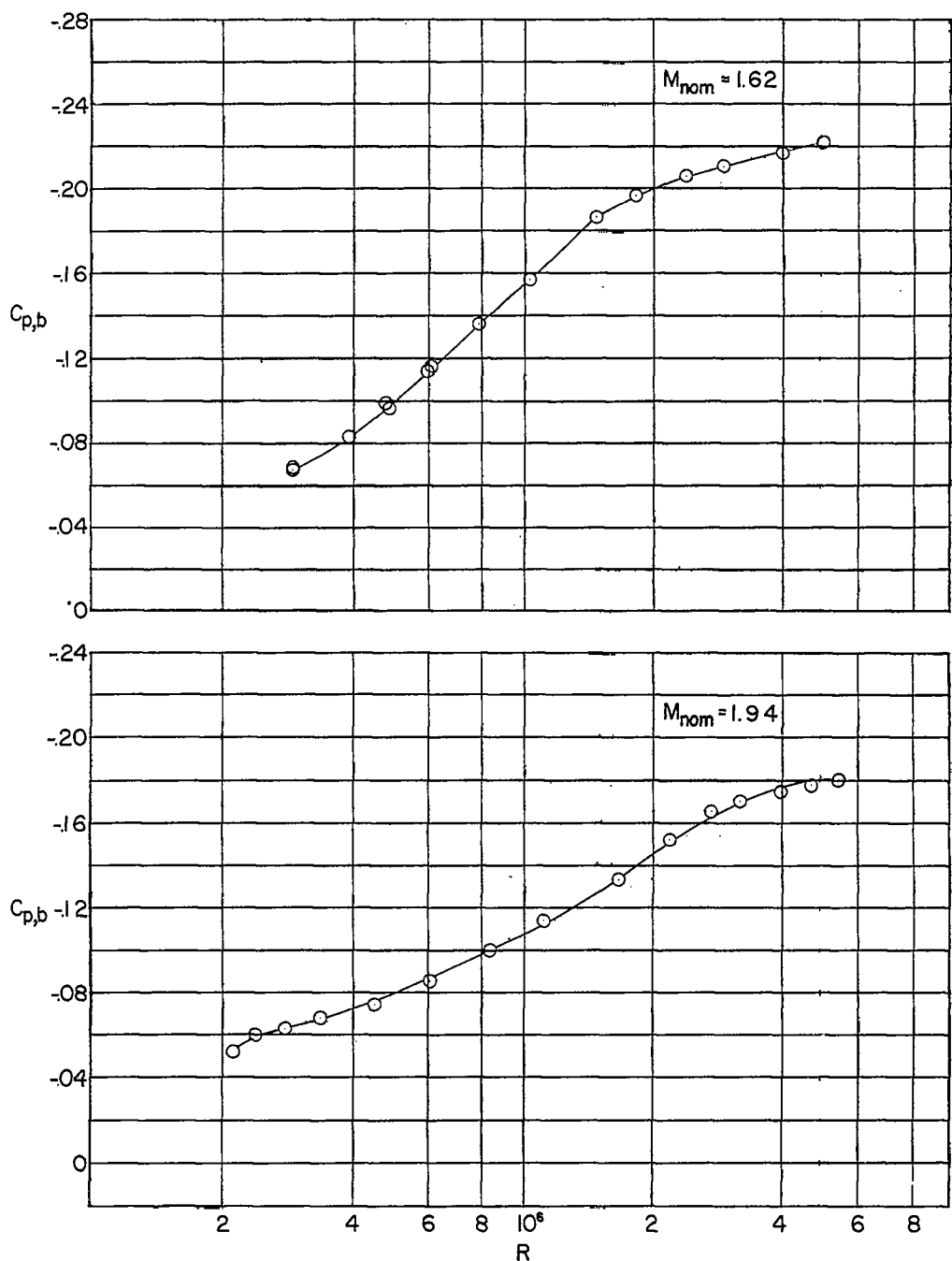
(e)  $l_m = 2.5$  inches.

Figure 8.- Continued.



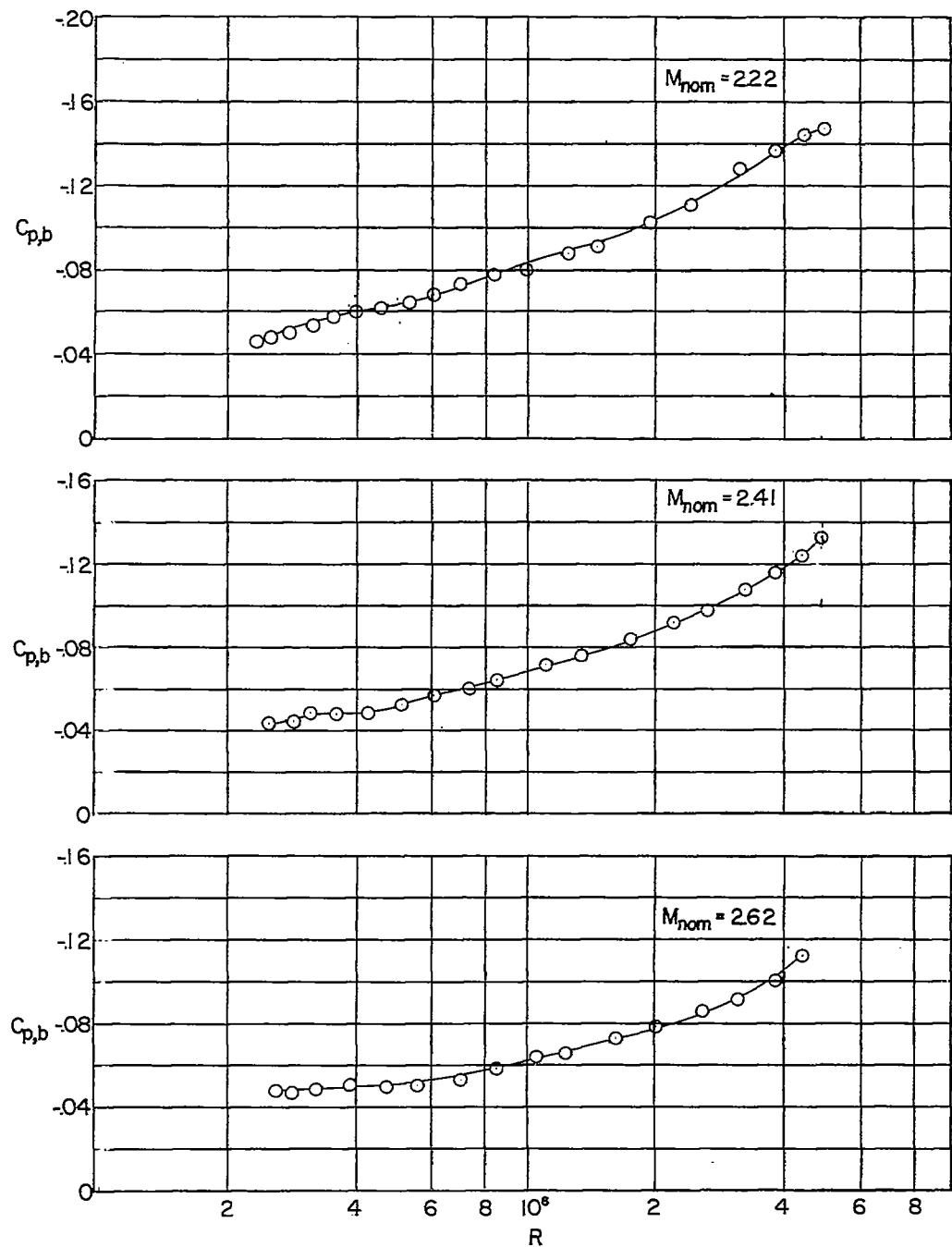
(e) Concluded.

Figure 8.- Continued.



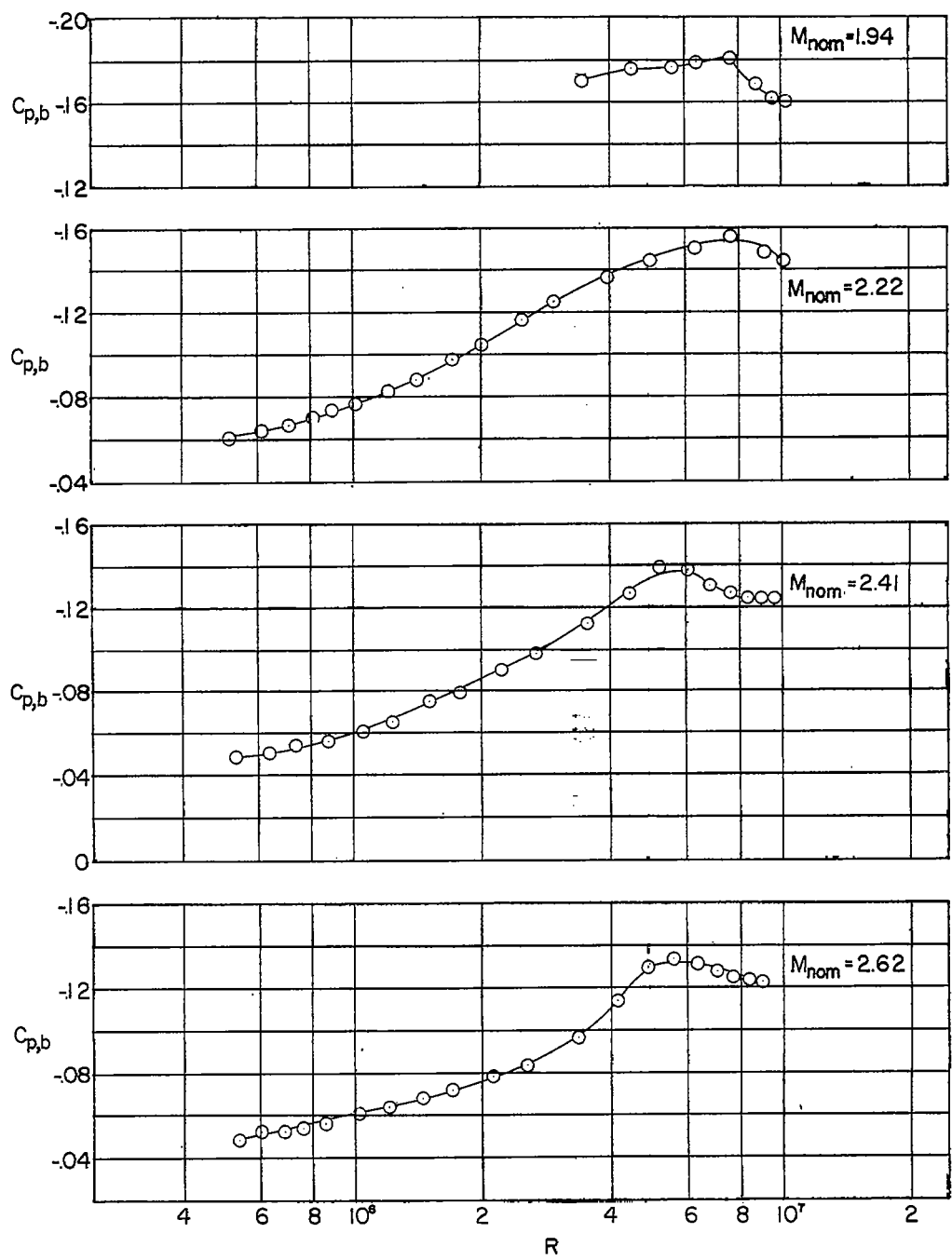
(f)  $l_m = 5.0$  inches.

Figure 8.- Continued.



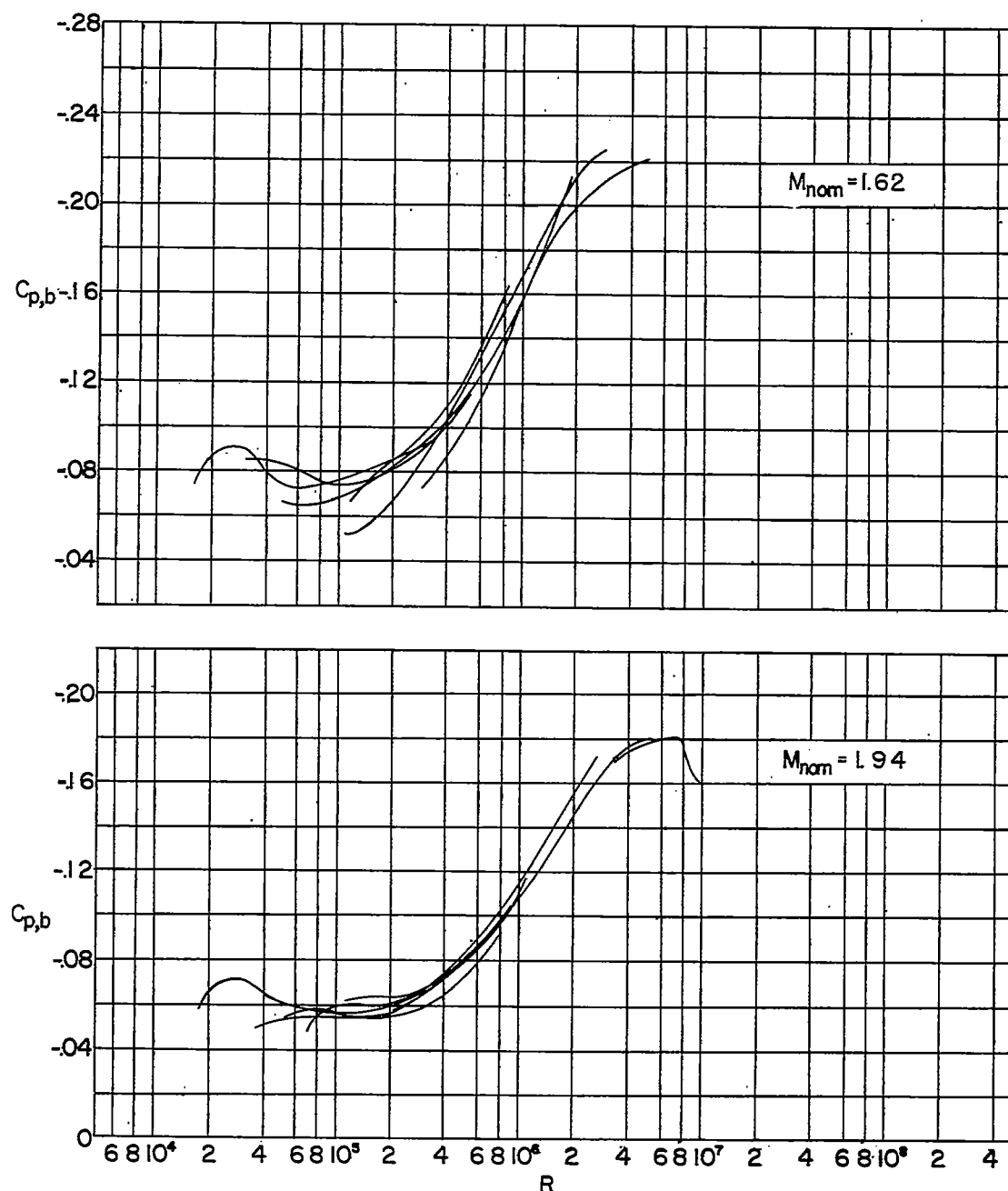
(f) Concluded.

Figure 8.- Continued.



(g)  $l_m = 10.0$  inches.

Figure 8.- Concluded.



(a)  $M_{\text{nom}} = 1.62$  and  $1.94$ .

Figure 9.-- Variation of base-pressure coefficient with Reynolds number with all models superimposed.

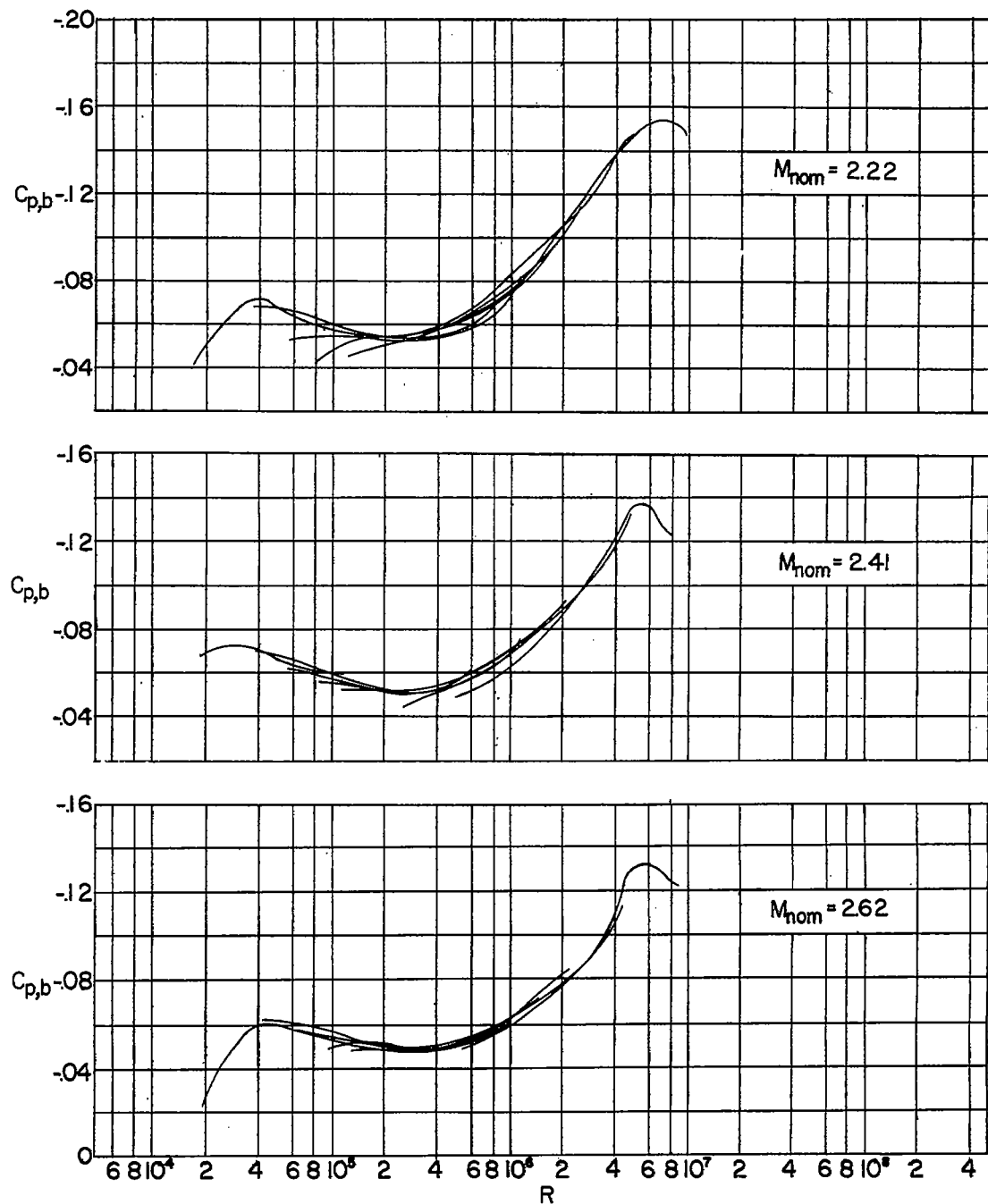
(b)  $M_{\text{nom}} = 2.22, 2.41$ , and  $2.62$ .

Figure 9.- Concluded.

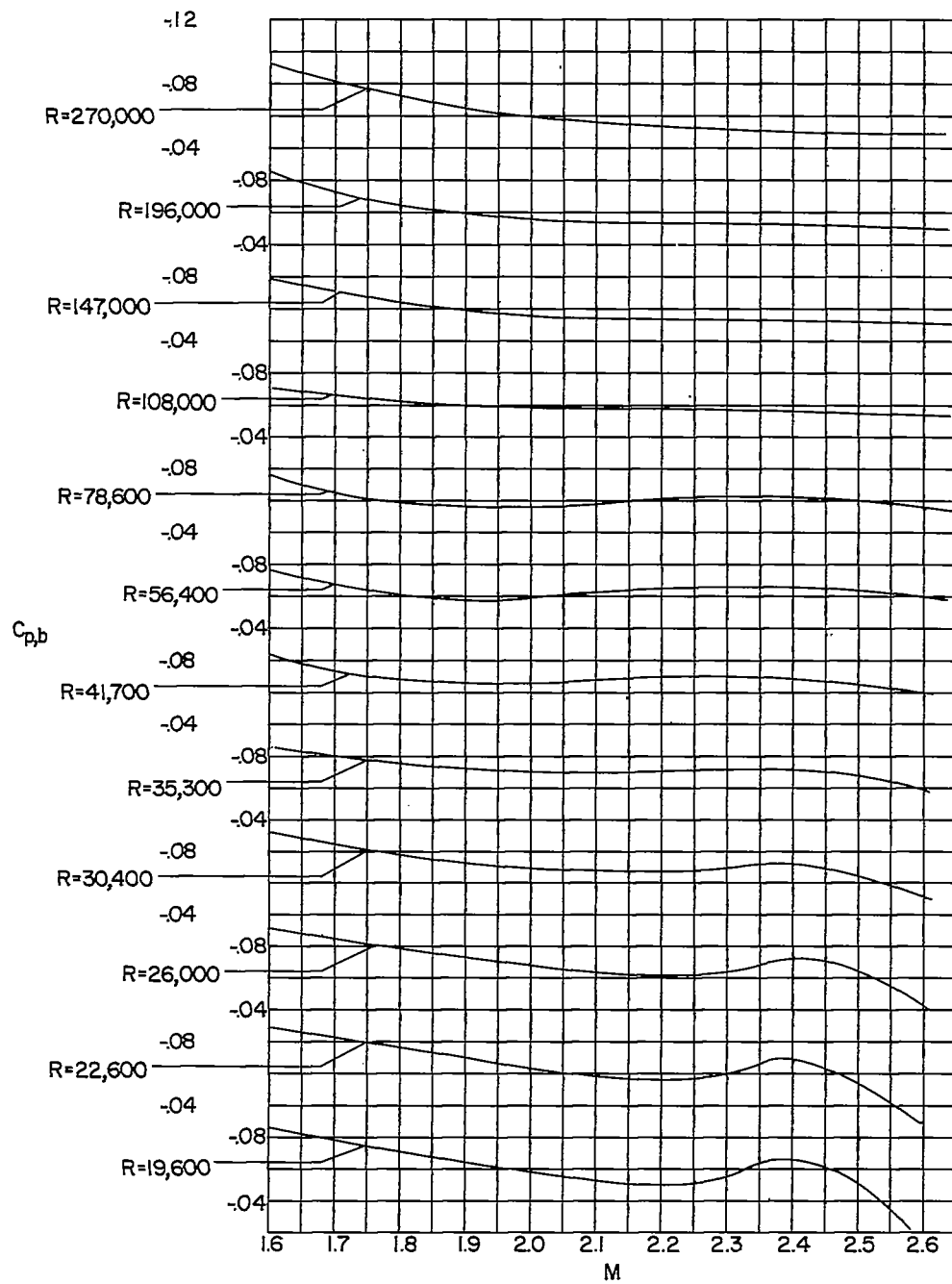
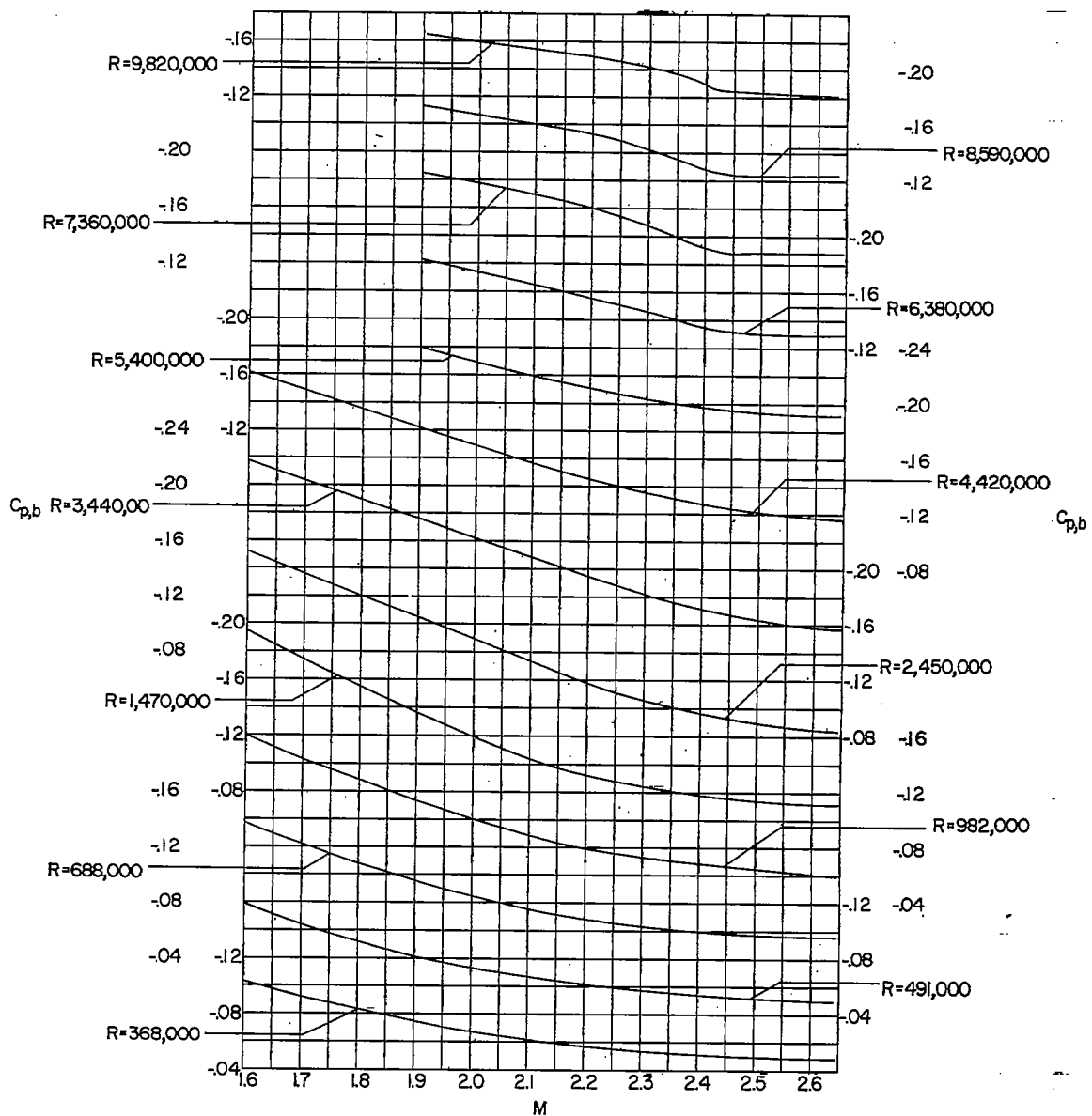
(a)  $R = 19,600$  to  $270,000$ .

Figure 10.- Variation of base-pressure coefficient with Mach number at constant Reynolds numbers.



(b)  $R = 368,000$  to  $9,820,000$ .

Figure 10.- Concluded.

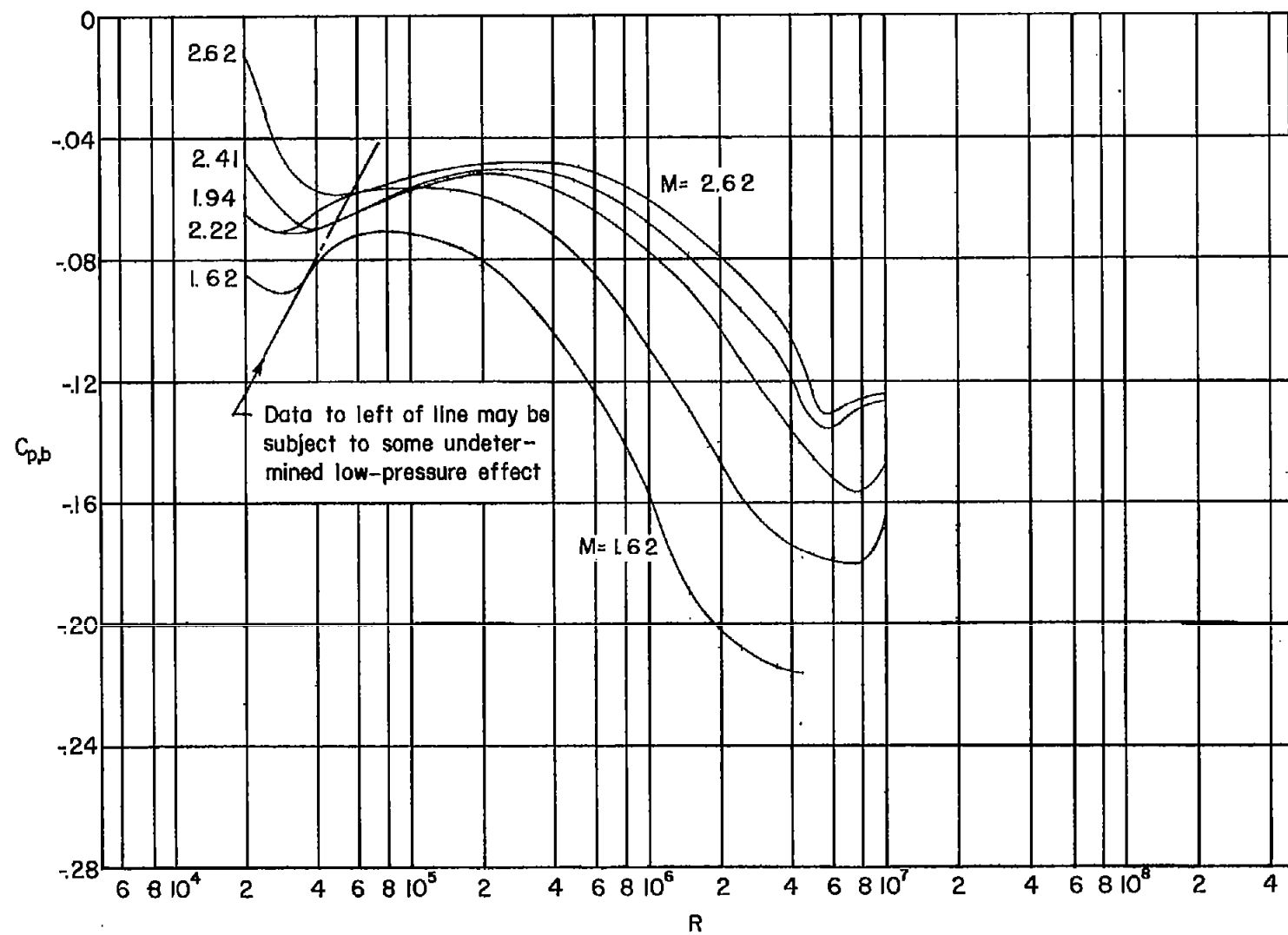


Figure 11.- Final curves of variation of base-pressure coefficient with Reynolds number.

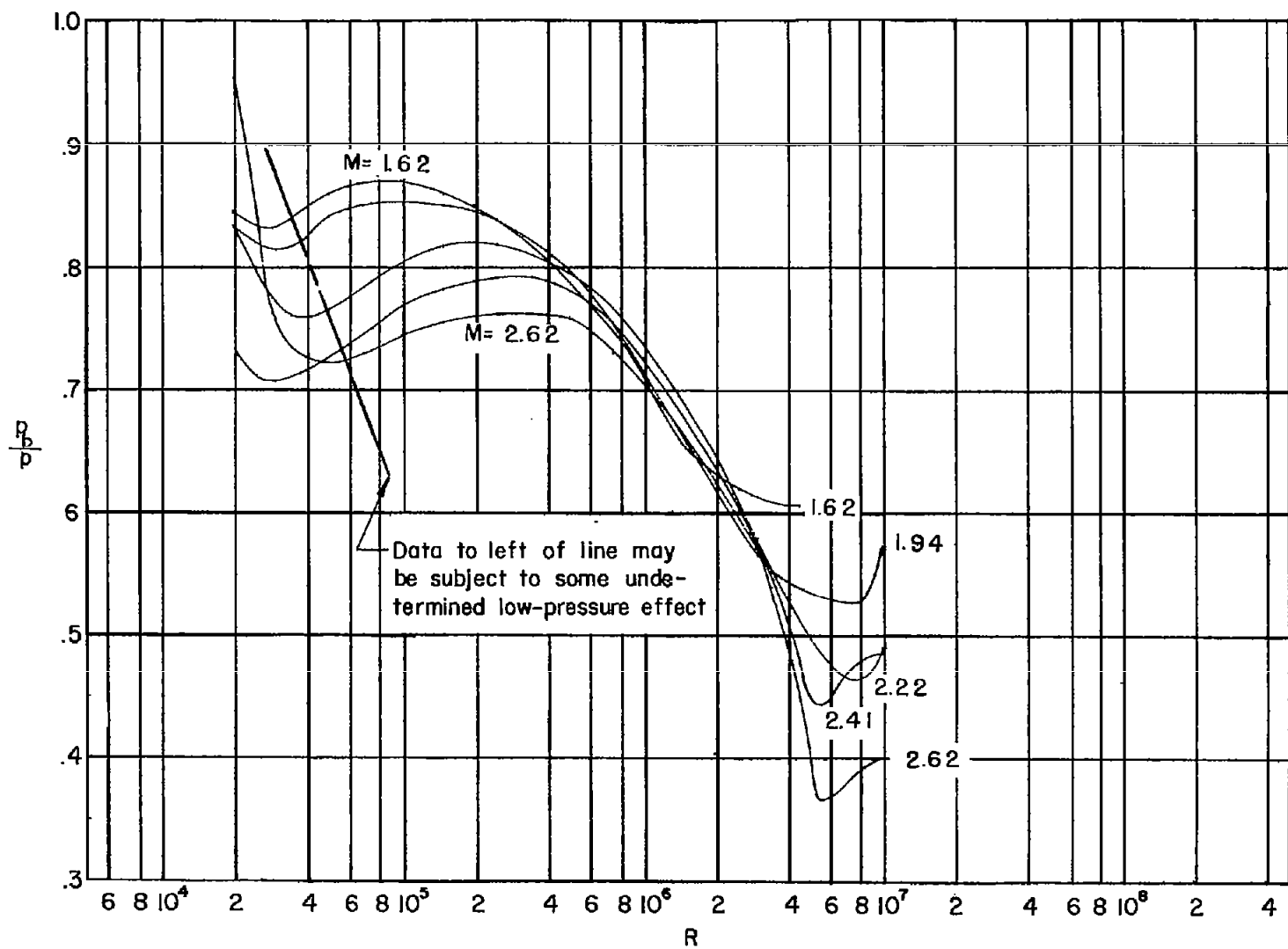


Figure 12.- Final curves of variation of pressure ratio  $p_b/p$  with Reynolds number.

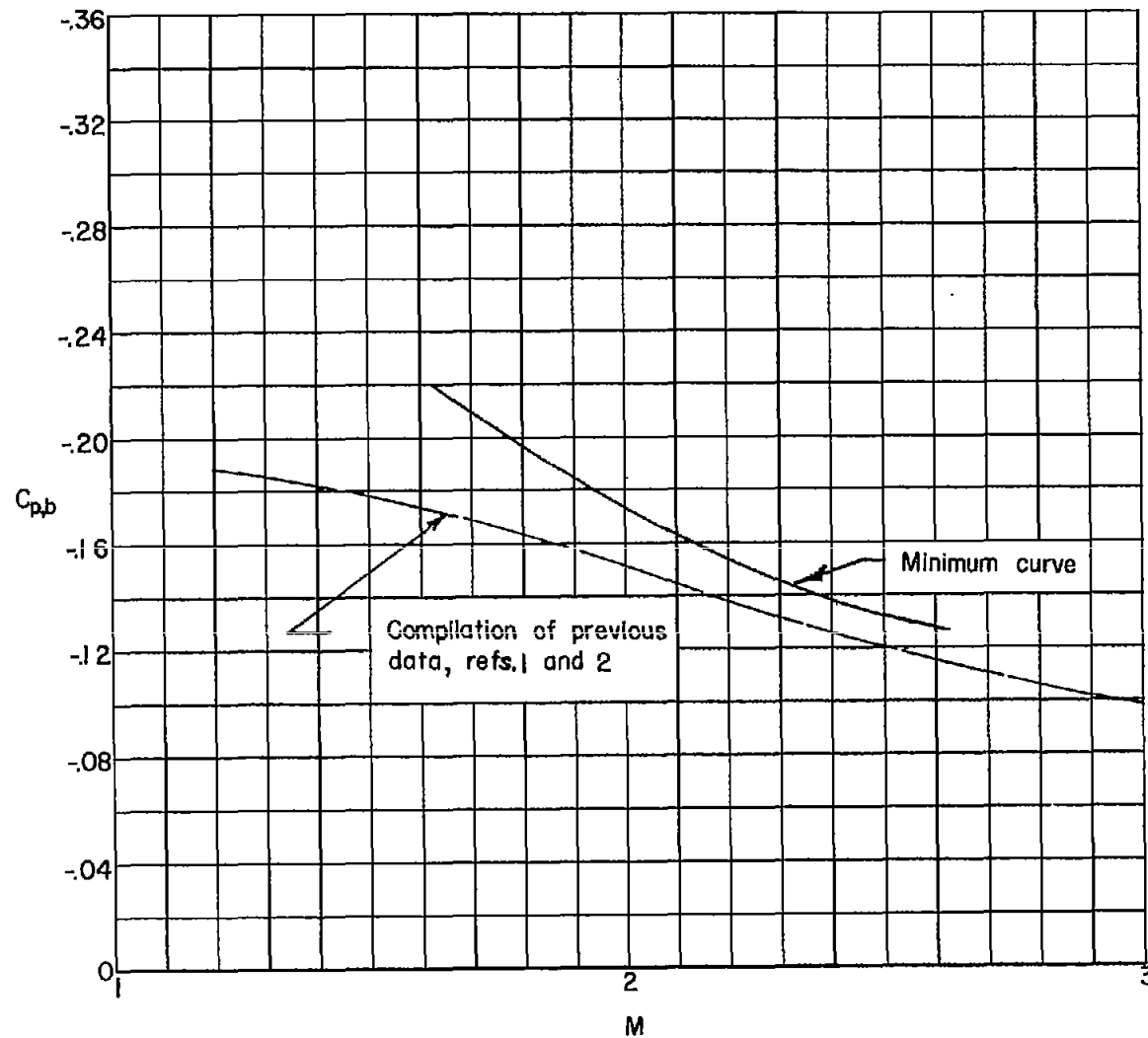


Figure 13.- Comparison of present data with previous data for variation of base-pressure coefficient with Mach number.

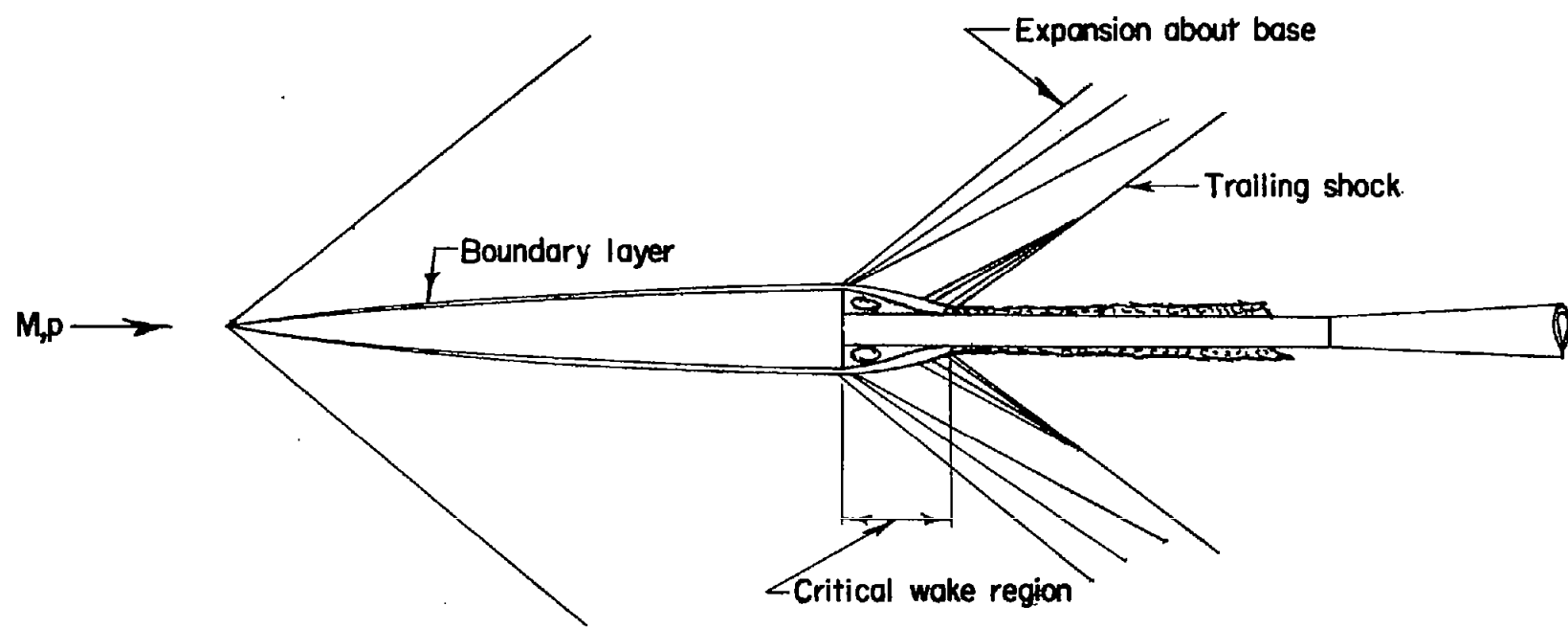


Figure 14.-- Schematic representation of flow over typical test model.

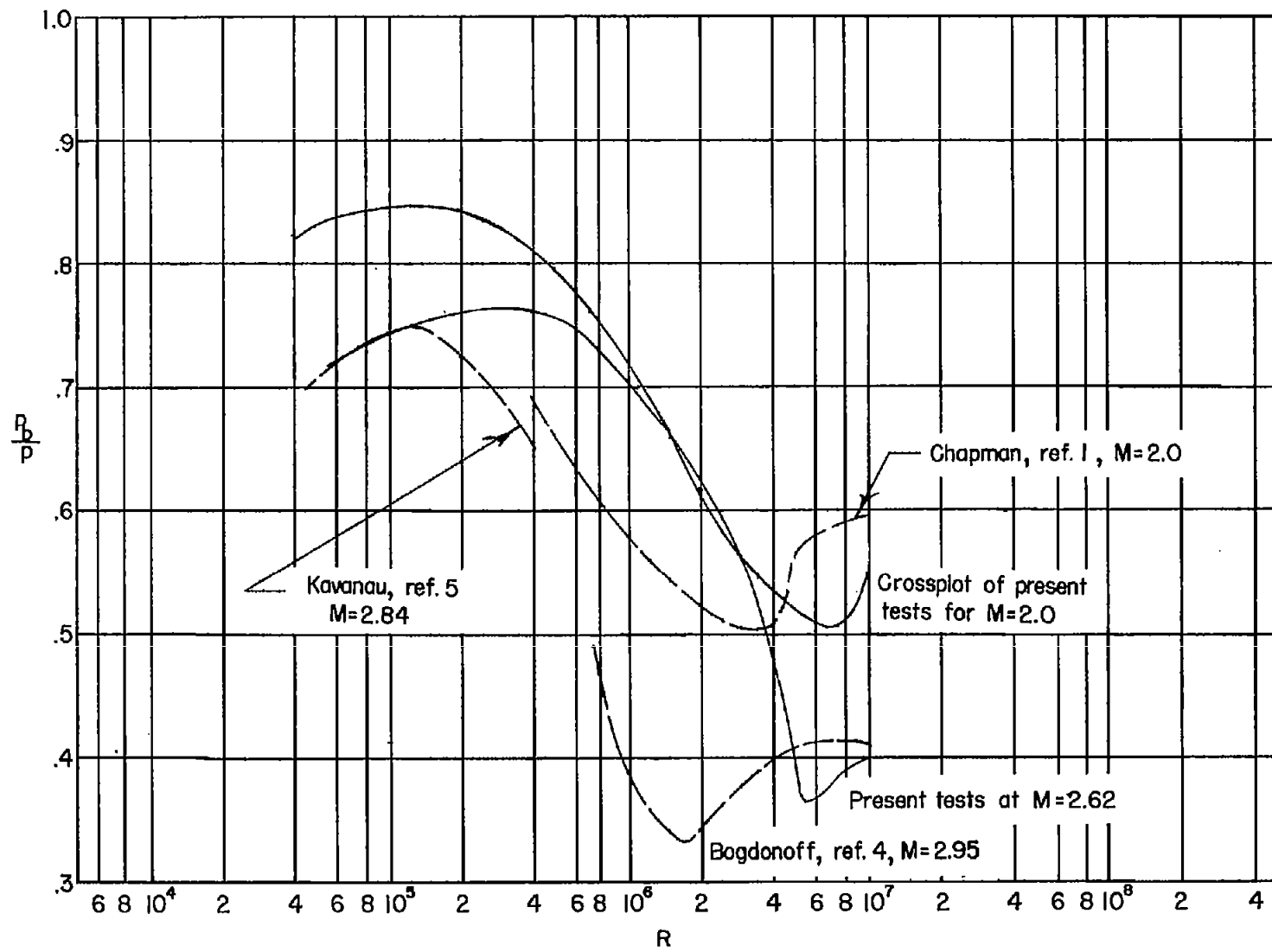


Figure 15.- Correlation of previous base-pressure data with those of present tests.